CHAPTER 2: Characterization of Uniform Mu *lipoxygenase 4* mutants for *Fv* resistance

Introduction

LOX pathway

Lipoxygenase (LOX)-derived metabolites named oxylipins are well known for their roles in biotic and abiotic stress responses. The LOX pathway begins when polyunsaturated fatty acids [linoleic (18:2) and linolenic (18:3) acid] are cleaved from cell membranes by diverse lipases and dioxygenated by either 9- or 13-LOX enzymes. Subsequent products from the 9- and 13-LOX reactions include either 18:2 derived (9S)- hydroperoxyoctadecadienoic acid (9-HPODE) and (13S)- hydroperoxyoctadecadienoic acid (13-HPODE) or the 18:3 derivatives (9S)-hydroperoxyoctadecatrienoic acid (9-HPOTE) and (13S)-hydroperoxyoctadecatrienoic acid (13-HPOTE). These hydroperoxides act as substrate for seven alternative branches of the LOX pathway, namely peroxygenases, divinyl ether synthases, reductases, epoxy alcohol synthases, hydroperoxide lyases (HPL), allene oxide synthases (AOS), and subsequent LOX reactions for the assembly of numerous oxylipins (Feussner and Wasternack, 2002). While there is yet much to unveil in terms of the physiological roles of plant oxylipins, current literature on wound and herbivory responses focused principally on the AOS and HPL pathway branches, responsible for the biosynthesis of jasmonic acid (JA) and green leafy volatiles (GLVs), respectively.

The synthesis of JA begins with LOX-derived 13-HPOTE, which is catalyzed into epoxides by AOS, transformed into a 5-carbon ring via allene oxide cyclase, reduced by 12-oxo phytodienoic acid reductase (OPR), and truncated by three beta-oxidation steps to form (+)-7-iso-JA (Wasternack, 2007). JA and/or its metabolites maintain a central role in herbivore induced defense responses. This is evident by the numerous studies conducted where JA is shown to have a regulatory influence on tritrophic interactions, resistance to phloem feeders, trichome-centered defenses, priming of indirect and direct defenses, pathogen resistance, and systemic defense signaling (Howe and Jander, 2008).

Similar to JA, the formation of the HPL-derived constituents begins with the cleavage of 13-HPOTE to form cis-3-hexenal, which is further enzymatically processed to produce other C6-compounds including cis-3-hexenol and cis-3-hexenyl acetate (Blée, 2002; D'Auria et al., 2002; Matsui, 2006). GLVs possess both anti-bacterial and anti-fungal properties, although some accounts show them to be fungal susceptibility factors when the fungus is exposed to lower levels of C-6 volatiles (Prost et al., 2005; Matsui, 2006). GLVs are known for their roles in herbivore defense.

While some studies show GLVs to be insect repellants (i.e. anti-HPL mutants in potato are more susceptible to aphids; Vancanneyt et al., 2001), GLVs can also increase a plant's herbivore appeal (i.e. anti-HPL mutants in tobacco are less attractive to Manduca sexta; Halitschke et al., 2004). GLVs are recognized as strong signaling molecules that regulate plant-plant communication after insect elicitation (Engelberth et al., 2004) and induce the expression of defensive genes (Bate and Rothstein, 1998). The exposure of maize plants to exogenous GLVs induces VOC and JA production, and more importantly, enhances the JA response to herbivore attack. These microbial and herbivore related examples show the large number of organisms that interact with GLVs and demonstrate the varied effects GLVs can have, based on the co- evolution of the plant and species involved. The specific signaling mechanisms behind JA- and GLV-mediated defense responses to wounding and herbivory are poorly understood, especially in maize. This may, in part, be a result of various technical challenges associated with LOXs being encoded by large multigene families, expressed in different tissues, producing different compounds, and regulated differentially by biotic and abiotic stresses. These facts alone are suggestive of their specialization in producing different oxylipins under different treatments and it is, therefore, likely that specific isozyme forms are responsible for providing substrate to specific pathway branches. For example, concerning multiple LOX isoforms found in tomato and potato, disruption of LOX-H1 and tomato TomLOXC show reduced levels of GLVs after tissue damage, but no changes in JA production (Leon et al., 2002; Chen et al., 2004). Alternatively, *Arabidopsis* AtLOX2 and tobacco NaLOX3 affect the JA biosynthetic pathway, yet forgo any function in GLV biosynthesis. Collectively, these studies show that diverse LOXs have specific functions, which may be a result of the intracellular spatial separation that exists between the different LOX pathways. Furthermore, these studies show that until now, the HPL and AOS branches of the LOX pathway have not been interdependent.

10-oxo-11-phytoenoic acid (10-OPEA) and 10-oxo-11,15- phyto-dienoic acid (10-OPDA) have been long considered candidates for biologically active compounds given their similarity to jasmonates (Hamberg et al 2000, Christensen et al 2015). Empirical findings in maize silks (Christensen et al. 2015) and a concurrent study done in maize roots (Ogorodnikova et al., 2015) showed that cis-10-OPEA synthesis in maize is consistent with full enzymatic biosynthesis, yielding predominantly (9S,13S)-10-OPEA as a result of an as-yet unidentified enzyme with novel 9-AOC activity. Together, these results suggest pathway diversity in 9-cyclopentenone formation between dicot and monocot species. One distinction from 12-OPDA activity is the weak ability of 10-OPEA to promote accumulation of transcripts coding for protease inhibitors. Furthermore, exogenous 10-OPEA application strongly induces cysteine protease activation and programmed cell

death, as evidenced by immunoblot protease labeling, lesion development, ion leakage, and DNA fragmentation (Christensen et al., 2015). Collectively, these results suggest that 9- and 13-LOX-derived cyclopentenones can have distinct and separate functions despite their structural similarities.

Classification and expression of lipoxygenase genes of maize (ZmLOXs)

A total of 13 different maize LOXs (*ZmLOXs*) with varying functions, localization, and regulation within the plant have been reported (Yan et al., 2012) and listed in Table 1.

Name	Gramene ID	Genebank accession	UniProt ID	Bin	Chr	Position[a] from	Position[a] to
ZmLOX1	Zm00001d042541 GRMZM2G156861	DQ335760	Q9LKL4	3.06	3	171,421,717 168,738,873	171,425,401 168,742,524
ZmLOX2	Zm00001d042540 GRMZM2G156861	DQ335761	A1XCH8	3.06	3	171,277,704 168.695,543	171,281,453 168,699,133
ZmLOX3	Zm00001d033623 GRMZM2G109130	AF329371	-	1.09	1	269,047,817 264,266,381	269,052,874 264,271,190
ZmLOX4	Zm00001d033624 GRMZM2G109056	DQ335762	M1HFG0	1.09	1	269,056,560 264,275,083	269,072,120 264,291,510
ZmLOX5	Zm00001d013493 GRMZM2G102760	DQ335763	A1XCI0	5	5	12,701,180 12,285,656	12,706,156 12,290,564
ZmLOX6	Zm00001d002000 GRMZM2G040095	DQ335764	A1XCI1	2.02	2	4,150,293 4,192,152	4,154,404 4,196,263
ZmLOX7	Zm00001d025524 GRMZM2G070092	DQ335765	A1XCI2	10.04	10	121,268,606 120,237,308	121,272,616 120,241,527
ZmLOX8	Zm00001d003533 GRMZM2G104843	DQ335766	A1XCI3	2.04	2	47,105,187 45,820,737	47,109,372 45,825,105
ZmLOX9	Zm00001d027893 GRMZM2G017616	DQ335767	A1XCI4	1.02	1	16,948,608 16,573,827	16,955,122 16,580,722
ZmLOX10	Zm00001d053675 GRMZM2G015419	DQ335768	A1XCI5	4.09	4	238,805,319 233,626,682	238,809,230 233,629,283
ZmLOX11	Zm00001d015852 GRMZM2G009479	DQ335769	Q06XS2	5.04	5	126,372,618 123,239,668	126,376,084 123,243,697
ZmLOX12	Zm00001d041204 GRMZM2G106748	DQ335770	A1XCI7	3.04	3	105,356,377 93,841,905	105,359,732 93,845,764
ZmLOX13	Zm00001d031449 GRMZM5G822593	-	-		1	190,316,537 188,148,388	190,321,767 188,153,483

Table 1. Column headers include Gramene ID, Genebank accession and UniProt ID (when available). Bin location indicates genetic mapping location according to maize GDB, and position (from and to) indicates the physical interval in relation to the B73 maize interference genome.

Four *ZmLOX* genes (*ZmLOX3*, GRMZM2G109130; *ZmLOX4*, GRMZM2G109056; *ZmLOX9*, GRMZM2G017616; and *ZmLOX13*, GRMZM5G822593, which was called *LOX2* in the previous B73 reference sequence annotation) were found on chromosome 1. *ZmLOX3* and *4* are only 3.7 kb apart; as such close proximity, neither QTL nor association mapping has a good possibility to distinguish the genetic effects of the two. Genes *ZmLOX6* and *8* (GRMZM2G040095 and GRMZM2G104843) are both located on chromosome 2. *ZmLOX1* (GRMZM2G156861 or ZM00001d042541), *ZmLOX2* (GRMZM2G156861 or ZM00001d042540) and *ZmLOX12* (GRMZM2G106748) are all found on chromosome 3. *ZmLOX1* and *2* are ~140 kb apart, and thus, the QTL mapping analysis will be unable to separate the effects; association mapping should, however. There is one gene on chromosome 4 (*ZmLOX10*, GRMZM2G015419). *ZmLOX5* and

ZmLOX11 (GRMZM2G102760 and GRMZM2G009479, respectively) are both located on chromosome 5. *ZmLOX7* (GRMZM2G070092) is located on chromosome 10. Furthermore, a summary of *LOX* gene expression in the different maize tissues is described in Table 2.

		Expression levels in uninoculated maize. Data from MaizeGDB gene expression atlas (Stelpflug et al., 2015)						
Gene Name	chr.	Anthers	Dev. ear	Endosp. 25 DAP	Ovule	Silk	Tassel	Pollen
ZmLOX1	3	2.5	51.6	13.6	242.1	39.5	15.2	0.01
ZmLOX2	3	2.5	51.6	13.6	242.1	39.5	15.2	0.01
ZmLOX3	1	14.2	14.9	9.9	37.2	5.8	57.4	0.03
ZmLOX4	1	10.3	32.4	2.1	54.9	19.9	21.3	0.39
ZmLOX5	5	25.5	194.2	5.3	549.3	557.5	180.1	0.06
ZmLOX6	2	0.5	85.5	13.3	197.3	26.0	113.6	0
ZmLOX7	10	6.9	0.4	0.9	0.7	0.4	1.6	0
ZmLOX8	2	4.3	3.0	2.2	2.0	3.1	13.6	0
ZmLOX9	1	9.5	16.4	3.1	6.2	18.9	3.2	0
ZmLOX10	5	0.3	33.1	6.4	132.1	669.1	53.4	0
ZmLOX11	3	1.5	0.3	22.4	8.1	0.2	2.3	0.51
ZmLOX12	1	0.7	0.1	0.1	0.2	0	1.8	0.04
ZmLOX13	1	-	-	-	-	-	-	-

Table 2. Expression data of *ZmLOX* genes in different maize tissues at different stages (Stelpflug et al., 2015). Tissue and stages include mature anthers, developing ear (Dev. ear), endosperm 25 days after pollination (Endosp. 25 DAP), mature ovule, silk, post-meiotic tassel, and pollen. The darker green intensity indicates higher expression levels.

There is evidence that ZmLOX8 and ZmLOX10 work synergistically, at least, in terms of wound-induced JA biosynthesis, although the genes are found on different chromosomes in the maize genome. A lack of expression of the GLV-producing ZmLOX10 leads to diminished levels of wound-induced expression of ZmLOX8, a major JA producing enzyme. Unfortunately, such an epistatic interaction could not be detected in the QTL mapping populations of the size used in this study. ZmLOX8 mapped directly under a QTL of LOD value 9.0. Biochemical analyses of lox10 knock-out mutants clearly showed that ZmLOX10 is the only LOX enzyme isoform required for production of GLVs (Gao et al., 2008). Interestingly, its closest segmentally duplicated homolog, ZmLOX11, is not involved in GLV biosynthesis as lox10 mutants are completely devoid of GLVs,

despite normally functioning ZmLOX11 (Christensen et al., 2013). This could be due to the lack of expression of *ZmLOX11* gene in mature maize leaves (Andorf et al., 2016).

ZmLOX10 was found beneath a QTL for aflatoxin accumulation resistance with a LOD value of 7.8; however, it was a large QTL interval and other genes may influence it as well.

ZmLOX5 belongs to the 9-LOX family and is expressed in silks, husk and tassel. It was mapped directly under another QTL found in bin 5.00 with a LOD value of 2.4. The near identical homolog ZmLOX4 was neither associated nor linked to a QTL for aflatoxin accumulation resistance, and it had a very different expression pattern than ZmLOX5, as it was expressed primarily in the roots (Christensen et al., 2011).

ZmLOX3 is expressed for the most part in the developing embryos, germinating seed and the innermost husk; no QTL for reduced aflatoxin in the ear was reported over this gene either.

Similar gene pairs ZmLOX7 and 8 showed alternate expression patterns, with ZmLOX7 expressed at very low levels overall, but slightly higher in the embryo and anthers, and ZmLOX8 expressed at high levels in older leaves. If ZmLOX8 is the causal gene for the strong QTL found directly above it, the phenotypic effect may be indirect, possibly even via interaction with ZmLOX10. On the other hand, similar gene pairs ZmLOX10 and 11 were both highly expressed in young leaves, but also in silks in the case of ZmLOX11 and older leaves in the case of ZmLOX10 (Andorf et al., 2016).

Maize Uniform Mu transposon mutants

Uniform Mu maize population was developed for genetics research. Its most notable features are the extent of its uniformity, and the degree to which this is punctuated by naturally-induced mutations from the Mu transposable elements within it. Uniform Mu maize is widely used for experimental analysis of gene function, since 1) the uniformity of the plants and seeds provides an excellent basis for comparison (controls), and 2) natural mutations of individual genes occur when the Mu transposable elements insert within them. Gene function can then be studied at the biochemical, metabolic, and whole-plant levels as a consequence of the specific changes in gene sequence. The altered genes are identified by a sequence-based approach (Uniform Mu database) and seeds are available to researchers (MaizeGDB and Stock Center).

Specific Uniform Mu mutants have been developed for *ZmLOX* genes. In particular, nine Uniform Mu mutants showed a mutation in different exons of the *ZmLOX4* gene and are listed in Table 3. Mu mutants showed a mutation in different exons of the *ZmLOX4* gene and are listed in Table 3. The stocks received corresponds to sib-pollinated F3 plants by the Maize Genetics COOP Stock Center of Urbana, Illinois. All UFMu stock collection are bronze-colored and homozygous for the

bronze-1 mu-mutable-9 (bz1-mum9) mutation used as a genetic marker for presence of MuDR, the autonomous transposable element of the Robertson's Mutator system (MuDR) (McCarty et al 2013). The *bz1-mum9* allele contains a non-autonomous Mu1 transposon insertion that disrupts the *Bz1* gene. *Bz1* encodes a UDP-glucose flavanol glucosyl transferase that catalyzes a key step in biosynthesis of purple anthocyanin pigment in the seed aleurone. All UFMu insertion lines in the public resource are screened for loss of Mutator activity using the *bz1-mum9* marker prior to sequence analysis in order to minimize occurence of non-heritable, somatic insertions in DNA samples used for sequence-indexing and mapping of germinal insertions. UFMu seed stocks deposited in the Maize Genetics Cooperation Stock Center have been carefully screened for absence of spotting as well as seed quality to ensure the insertion lines are genetically stable and no longer Mu-active.

UFMu *lox4*	insertion according ATG
UFMu10924	5’
UFMu12283	5’
UFMu06517	5’
UFMu08535	5’
UFMu3075	5’
UFMu3258	5’
UFMu01831	3’
UFMu11880	3’
UFMu5366	3’

Table 3. List of *lox4* Uniform Mu transposon mutants available in our laboratory.

Selection of the candidate gene ZmLIPOXYGENASE4 and involvement in the defense response towards Fv

The expression analysis of the *ZmLOX4* (GRMZM2G109056) gene was previously investigated in the work by Maschietto et al. (2015). The expression profile of fifteen genes of the LOX pathway (including *ZmLOX4*) was studied in kernels of the resistant (R) and susceptible (S) lines at different times after *Fv* inoculation. It was observed that the expression of *ZmLOX3*, *ZmLOX4, LOX6* and *ZmLOX12* genes was enhanced in the R line at 7 days post inoculation (dpi), with FC values of 4.4, 11.3, 39.9 and 54.9, respectively, and then, strongly decreased at 14 dpi. In the S line, lower FCs were measured for all *LOX* genes over the time-course considered (Maschietto et al., 2014). In

addition, all genes resulted overexpressed before the infection in kernels of the resistant genotype already at 3 dpi, suggesting that resistance in maize may depend on the earlier activation of these genes. Similarly, *ZmLOX4* resulted strongly up-regulated in maize kernels under field condition at 4 dpi with a further mycotoxigenic pathogen, *Aspergillus flavus* (Dolezal et al., 2014). These findings highlight the crucial role of *ZmLOX4* and in general of all *ZmLOX* genes in plant-pathogen cross-talk. The employment of maize mutants (Christensen et al., 2013; 2014; Gao et al., 2014) and *Fv* mutants (Lanubile et al., 2013; Scala et al., 2014; Battilani et al., 2018) helped to clarify the role of LOX and jasmonic acid (JA) in the resistance mechanisms against *Fv*. Maize *lox3* mutants have shown that the 9-LOX pathway controls plant germination, root growth and senescence (Gao et al., 2008a) and contributes to maize resistance to *Aspergillus* spp. (Gao et al., 2009) and susceptibility to several fungal pathogens, including *Fv* (Gao et al., 2007). On the other hand, *Lox12* mutant was more susceptible to *Fv* colonization of mesocotyls, stalks and kernels and fumonisin contamination of the kernels, showing diminished levels of jasmonates and expression of genes of the JA-biosynthetic pathway (Christensen et al., 2014). Despite a remarkable number of publications on the *lox3* and *lox12* maize mutants, few information are available for *lox4* mutants. For this reason, the characterization of this mutant was carried out in this PhD work to better explain the maize host resistance to *Fv*.

A further *ZmLOX* candidate gene was the plastidial *ZmLOX6* that represents a novel *LOX* subfamily, distinct from 9- and 13-LOXs previously characterized, able to metabolize the 13-LOX-derived fatty acid hydroperoxides (Gao et al., 2008b). In Maschietto et al. (2015) work *ZmLOX6* was subjected to a moderate up-regulation in both genotypes at 3 and 7 dpi, and its induction resulted almost eight times greater in inoculated S at 14 dpi in comparison to R. Since this gene was not responsive to wounding or insects, but was induced by JA and to *Cochliobolus carbonum*, it may contribute to susceptibility to this pathogen (Gao et al., 2008b) and also to *Fv*, as evinced by Maschietto et al. (2015). *ZmLOX6* was selected in our work as a good candidate gene for *Fv* resistance. Due to the lack of Uniform Mu transposon population for this gene the CRISPR-Cas9 genome editing approach was applied to characterize *ZmLOX6* and evaluate its implication in the defense responses to *Fv*, as further discussed in the CHAPTER 3 of this thesis.

Aim of the work

It is known that plant lipoxygenase (LOX)-derived oxylipins regulate defense against pathogens and that the host-pathogen lipid cross-talk influences the pathogenesis. In this regard, maize mutants carrying Mu insertions in the *ZmLOX4* gene (named as UFMu*lox4*), together with other two maize genotypes, the susceptible W22 and the resistant TZI18 lines, were tested for *Fv* resistance by the screening method rolled towel assay (RTA). This *in vivo* assay shows high reproducibility and specificity in evaluating the ability of different pathogens to infect and colonize seedlings. RTA was extensively applied in soybean to evaluate seedling resistance to *Fusarium graminearum* and the aggressiveness of different *Fusarium oxysporum* isolates, and it was adapted to the maize-*Fv* pathosystem. The same lines evaluated for *Fv* resistance after RTA were analyzed for their content of fumonisins. Additionally, the expression profiles of 16 genes involved in the LOX pathway were studied and the lipoxygenase activity was also investigated in the same lines. Furthermore, UFMu*lox4*, W22 and TZI18 were evaluated for *Fv* resistance by mechanical inoculation in field in order to validate the previous results obtained by RTA at seedling stage.

Results and Discussion

PCR confirmation of Mu insertion

To confirm the presence of the Mu insertions in the *ZmLOX4* gene, genomic DNA was extracted from individual UFMu*lox4* plants and analyzed by PCR using gene-specific primers and sequencing. A scheme of the gene *ZmLOX4* and UFMu insertions and positions are shown in Figure 1 and Table 4.

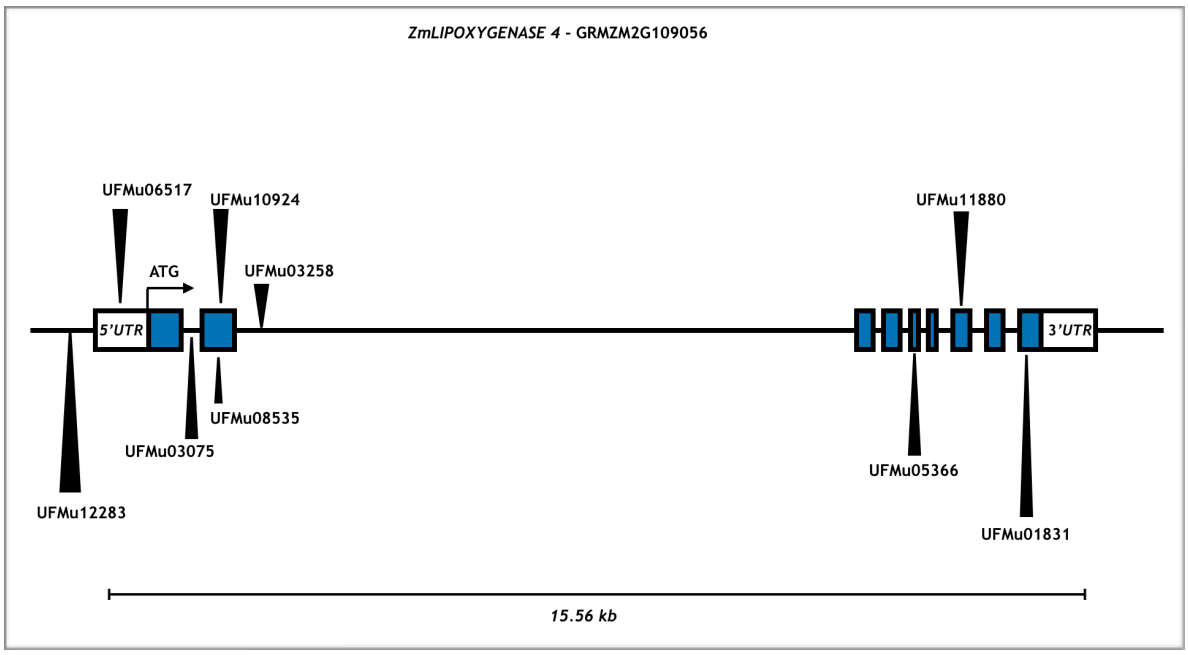

Figure 1. *ZmLOX4* gene map and UFMu insertions.

Lox4 UFMu alleles placed between the *LOX4* promoter and the beginning of the second intron were selected for the further analysis. The choice of these mutants was due to the higher probability of obtaining a truncated protein during the translation, when the transposon is located closed to the ATG. For this reason, the alleles UFMu12283, UFMu06517, UFMu03075, UFMu10924, UFMu08535 and UFMu03258 were sequenced as shown in supplemental data paragraph at the end of this chapter (Table SD1). The absence of the transposable element MuDR in the *bz1-mum9* allele was confirmed. When active MuDR is present in the genome, transposition of the Mu1 element in *bz1-mum9* is induced in somatic tissues of the endosperm resulting in a spotted aleurone phenotype. The spots are due to small, typically single-cell, revertant sectors that produce purple anthocyanin. All nine mutants were screened for disease phenotyping by RTA, but the most uniform allele UFMu10924 has been chosen for the further characterization of the *ZmLOX4* gene according to

sequencing and MuDR phenotype. UFMu*lox4* mutants were reproduced in field last 2017 (Figures 2 and 3).

Table 4. UFMu insertion point in *ZmLOX4*. Sequences available at the end of the chapter for the yellow alleles with MuDR from promoter to the second intron.

UFMu lox4	insertion according ATG	sequence code	field code 2017
UFMu10924	+ 935 bp	FR07686682	570
UFMu12283	- 204 bp - promoter region	FR07686683	571
UFMu06517	-52 bp - 5'UTR	FR07686686	572
UFMu08535	+ 1045 bp - exon 2	FR07686696	573
UFMu03075	+ 717 - intron 1	FR07686692	575
UFMu03258	+1131 bp - intron 2	FR07686690	576
UFMu01831	exon 9	-	566
UFMu11880	exon 7	-	568
UFMu05366	exon 5	-	569

Figure 2. Reproduction of UFMu*lox4* plants in Cerzoo experimental farm set in Piacenza, Italy.

Figure 3. Ears of UFMu*lox4* 10924 (left) and 03258 (right).

Disease phenotyping by RTA

All nine UFMu*lox4* mutants were tested for *Fv* resistance by RTA (Table 4). TZI18 and W22 were used as resistant and susceptible control lines as previously reported in Stagnati et al. (unpublished data). Beside disease severity evaluation caused by *Fv*, seedling weight and length were measured 7 day after *Fv* infection. Examples of control and treated seedlings after RTA are shown in Figure 4 for *TZI18*, *lox4 UFMu10924*, *lox4 UFMu03258*, and *W22*.

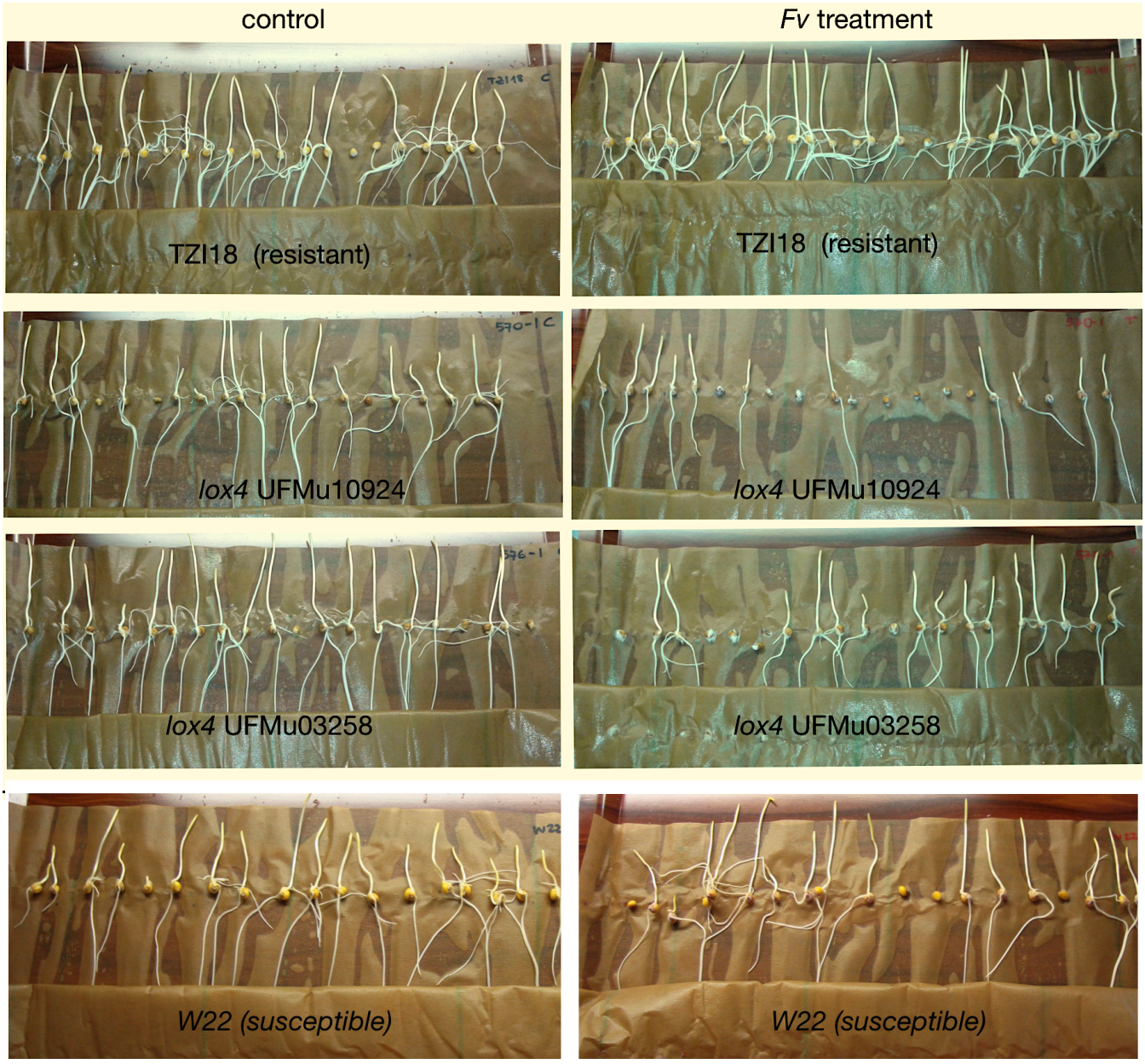

Figure 4. RTA after 7 days of inoculation with *Fv*. Comparison of two inbred lines and two mutants: TZI18 (resistant inbred line), UFMu*lox4 10924*, UFMu*lox4 03258*, and W22 (susceptible inbred line). Left side: control treatment (seeds inoculated with water); right side: *Fv* treatment.

The whole results of all nine UFMu*lox4* mutants are reported in Figure 5 together with the results reported for TZI18 and W22 lines. Generally, no statistical differences in plant weight (gr) are reported, while differences in length and disease severity are more evident. Small differences were observed for length (cm) in TZI18 control and treated seedlings, whilst W22 and UFMu*lox4* showed a decrease in plant length after treatment. The latter ones also displayed the highest disease severity values after *Fv* inoculation with values of 3.20 and XX, respectively (devi inserire anche il valore della W22 che mi sembra sui 2,5 circa) after treatment. These findings confirm the resistance of the TZI18 line in comparison to W22, and highlight how the UFMu*lox4* mutants represent susceptible materials to *Fv* infection, confirming the role of *ZmLOX4* gene in maize resistance (Dolezal et al., 2014; Maschietto et al., 2015). A complete table of RTA and the related analysis performed is shown in supplemental data paragraph (Table SD1).

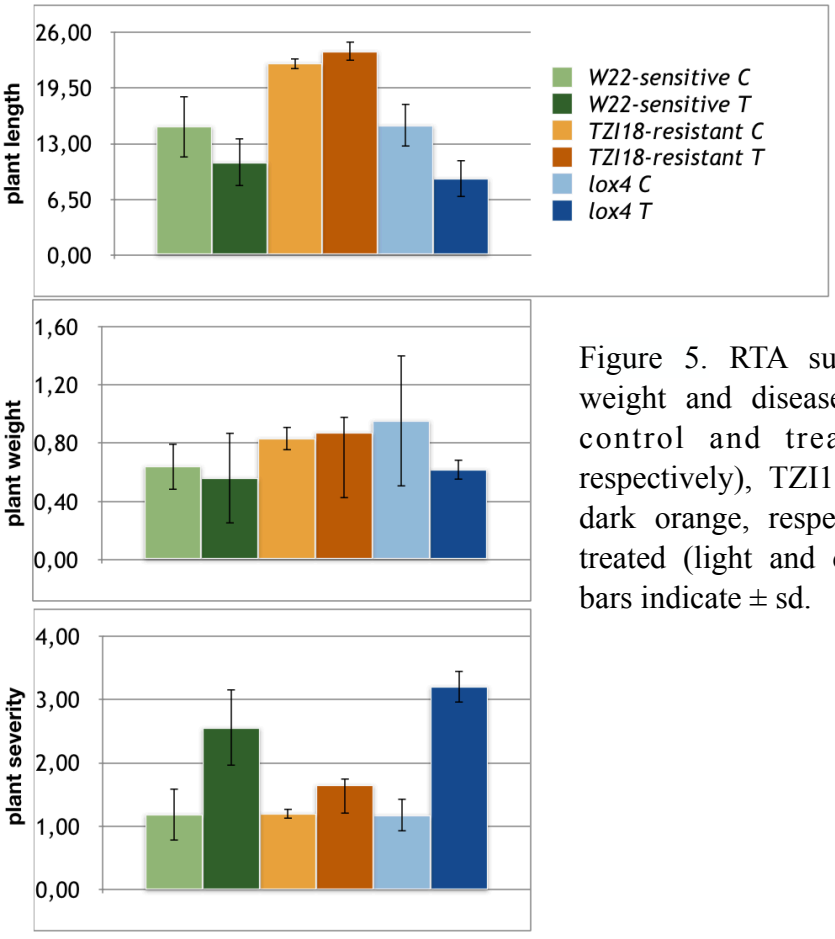

Figure 5. RTA summary results of plant length, weight and disease severity in seedlings of W22 control and treated (light and dark green, respectively), TZI18 control and treated (light and dark orange, respectively), UFMu*lox4* control and treated (light and dark blue, respectively). Vertical bars indicate ± sd.

Analysis of the fumonisin content

The resistant (TZI18) and the susceptible (W22) lines, and two UFMu*lox4* mutants (10924 and 03258) were also characterized for the content of total fumonisin (B1, B2 and B3) seven days after *Fv* infection by RTA. Fumonisin analysis was performed by an ELISA Kit based on the principle of the enzyme linked immunosorbent assay and data are shown in Figure 6 and Table SD2 in supplemental data paragraph. All samples showed very low levels of fumonisin in control condition. As expected, higher levels of fumonisins were measured in the treated samples and clear differences were found between the resistant line TZI18 (5.1 ppm) compared to the susceptible W22 (45,46 ppm) and UFMU*lox4* mutants, with UFMu10924 reaching the highest content of about 63 ppm of total fumonisin. These results collectively demonstrated the resistance of the TZI18 line, as highlighted by a limited growth of the pathogen (Figure 5) and the low fumonisin content (Figure 6). Furthermore, the impaired functionality of the *LOX4* gene seriously compromised the host resistance to *Fv*, as already reported by Park et al. (2010) and Battilani et al. (2018).

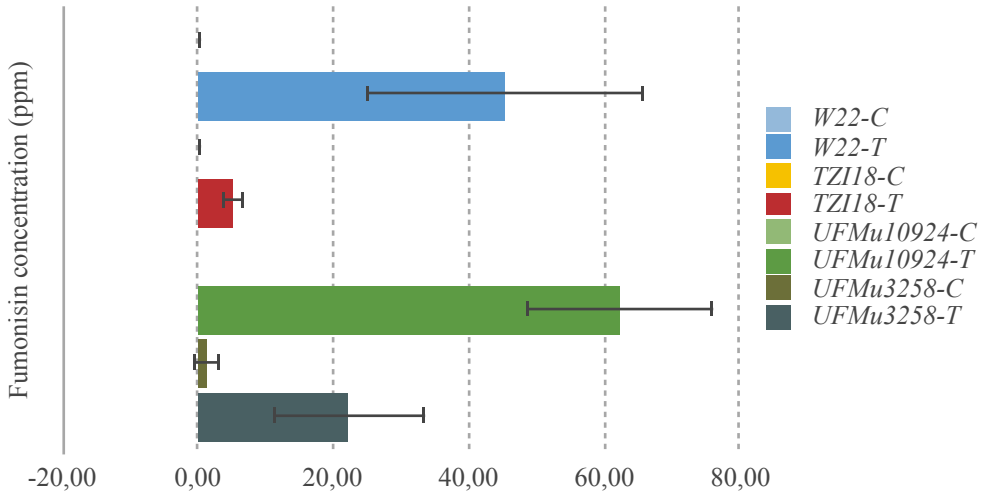

Figure 6. Total fumonisin content of FB1, FB2 and FB3 in W22, TZI18 and UFMu10924 and UFMu3058 mutants.

Regulation of the expression of maize LOX and GLV genes

In this work the expression levels of four selected 9-LOX genes, *ZmLOX3*, *ZmLOX4*, *ZmLOX5* and *ZmLOX12*, four selected 13-LOX genes *ZmLOX7*, *ZmLOX8*, *ZmLOX10* and *ZmLOX11*, the plastidial *ZmLOX6*, and further seven genes for the biosynthesis of green leaf volatiles (GLV) and jasmonates (*ZmAOS*, *ZmHPL*, *ZmOPR8*, *ZmAOX*, *ZmLBP*, *Zmplt*, *ZmOPCL*) were measured by real-time RT-PCR. In order to establish the strength of induced defense responses determined by *Fv* in the two maize lines TZI18 and W22, and in the mutant UFMu*lox4*, the FCs were calculated as transcript content of treated TZI18 (resistant) over treated W22 (susceptible); treated TZI18 (resistant) over treated UFMu*lox4* (susceptible); treated W22 (susceptible) over treated UFMu*lox4* (susceptible) (Figure 7a and b). Furthermore, FCs were calculated also as transcript content of treated over control sample of each inbred (Figure 8a and b). The most representative mutant allele of UFMu*lox4* (UFMu10924) was considered for the gene expression analysis by real-time RT-PCR. The results showed that TZI18 had higher levels of expression for almost all genes compared to the susceptible W22 and UFMu*lox4*, and this was more evident for the mutant for both LOX and GLV pathway (Figure 7a and b). Taking in account each single line after *Fv* treatment, the strongest up-regulation was observed for the resistant line TZI18, in particular for the gene *ZmLOX6* (FC=29,75), and *ZmLOX11* (FC=44.70) (Figure 7a). As regards the GLV pathway, the most responsive gene was *ZmOPR8* (FC=16,82), followed by *ZmHPL* (FC=25,09) (Figure 7b). As reported in Maschietto et al. 2015, *ZmOPR8* was still overexpressed in resistant lines, as *ZmAOS ZmOPLC, ZmAPX* and *ZmHPL*. *ZmOPR* are OPDA reducatases involved in peroxisome beta-oxidations and their expression is increased in resistant lines as confirmed in our study and in Maschietto et al. 2015. Gene expression analysis reports the same pattern for *ZmHPL* a Lipid Transfer Protein (LPT) that recruit membrane lipids and performed multiple roles in pathogen defense and plant growth (Yeats and Rose, 2008). In *lox4* mutant we can confirm that *ZmOPR* and *ZmHPL* genes are involved in defense because the susceptible pattern of *lox4* shows a big decrease in *ZmOPR* and *ZmHPL* expression compared to the resistant line. Very low expression of *ZmLOX4* in the mutant UFMu*lox4* confirming the exon deletion and the absence of mRNA. The down-regulation of most LOX and GLV genes in the mutant, as well as the high level of disease severity observed by RTA, proved the previous findings by Battilani et al. (2018), where two knockout alleles for *ZmLOX4* displayed dramatically increased fungal growth and conidia production compared with its respective near-isogenic WT line. These results provide genetic evidence that *ZmLOX4* gene is essential for seed defense against *Fv*.

Gene expression results - FC in treated samples

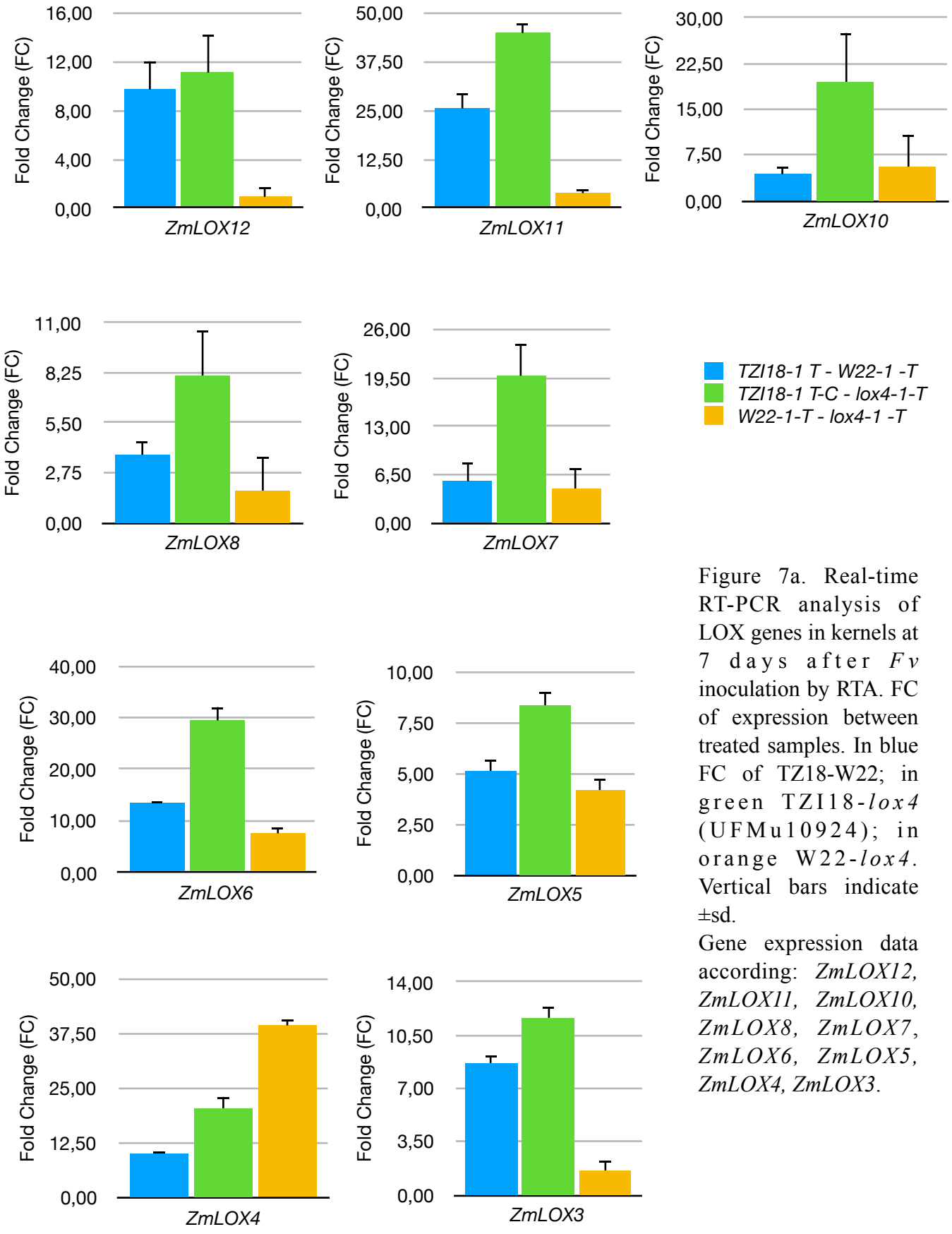

Figure 7a. Real-time RT-PCR analysis of LOX genes in kernels at 7 days after *Fv* inoculation by RTA. FC of expression between treated samples. In blue FC of TZ18-W22; in green TZI18-*lox4* (UFMu10924); in orange W22-*lox4*. Vertical bars indicate ±sd.
Gene expression data according: *ZmLOX12, ZmLOX11, ZmLOX10, ZmLOX8, ZmLOX7, ZmLOX6, ZmLOX5, ZmLOX4, ZmLOX3*.

Gene expression results - FC in treated samples

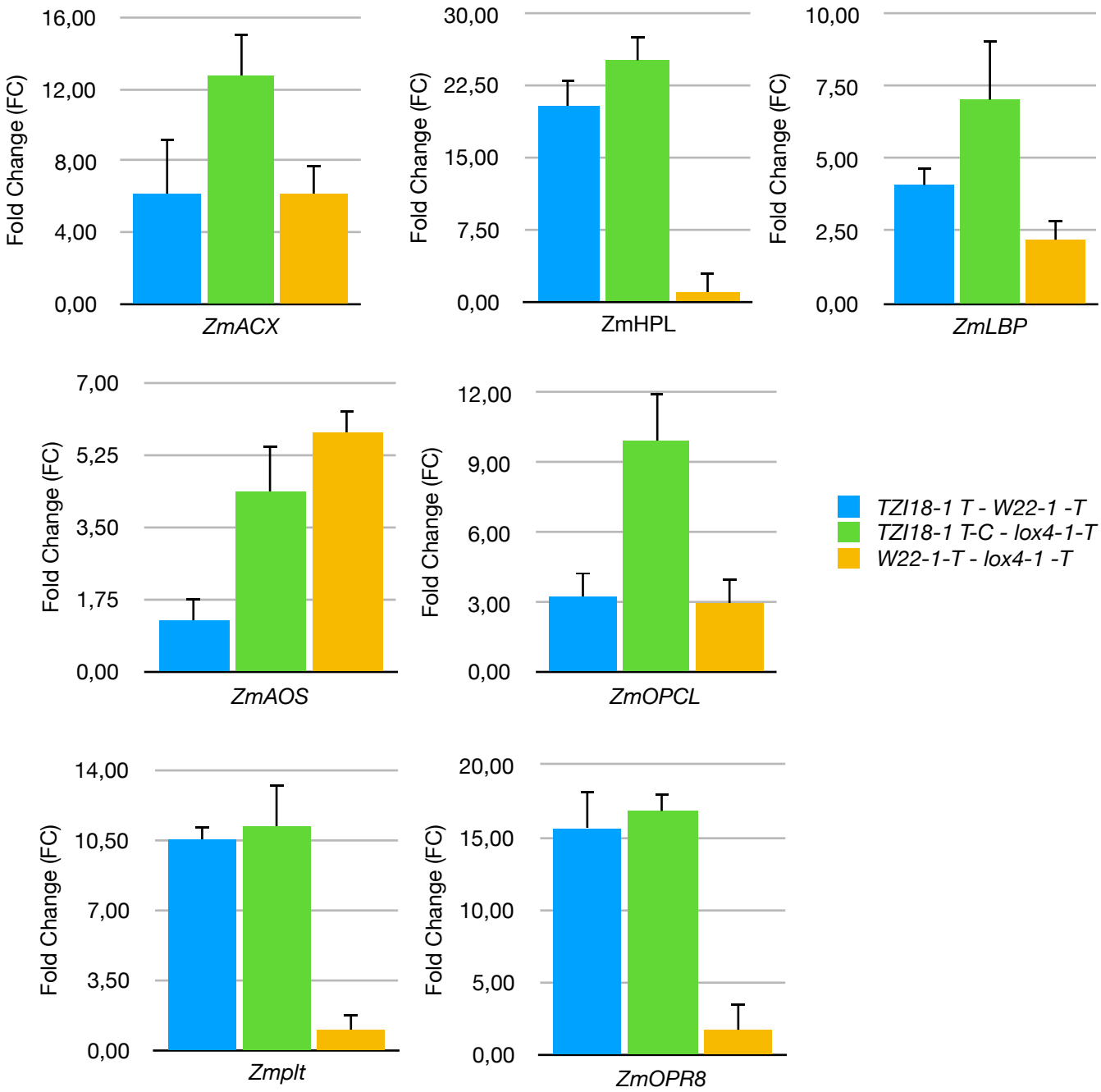

Figure 7b**.** Real-time RT-PCR analysis of GLV genes in kernels at 7 days after *Fv* inoculation by RTA. FC of expression between treated samples. In blue FC of TZ18-W22; in green TZI18-lox4 (UFMu10924); in orange W22-lox4. Vertical bars indicate ±sd. Gene expression data according: *Zm allene oxide synthase (ZmAOS)*, *Zm hydroperoxide lyase* (*ZmHPL)*, *Zm OPDA reductase8* (*ZmOPR8*), *Zm acyl-CoA oxidase,* (*ZmACX), Zm lipid binding protein* (*ZmLBP)*, *Zm phospholipid transfer protein,* (*Zmplt*), *OPC-8:0CoA ligase1* (*ZmOPCL)*.

Gene expression results - FC treated over control samples

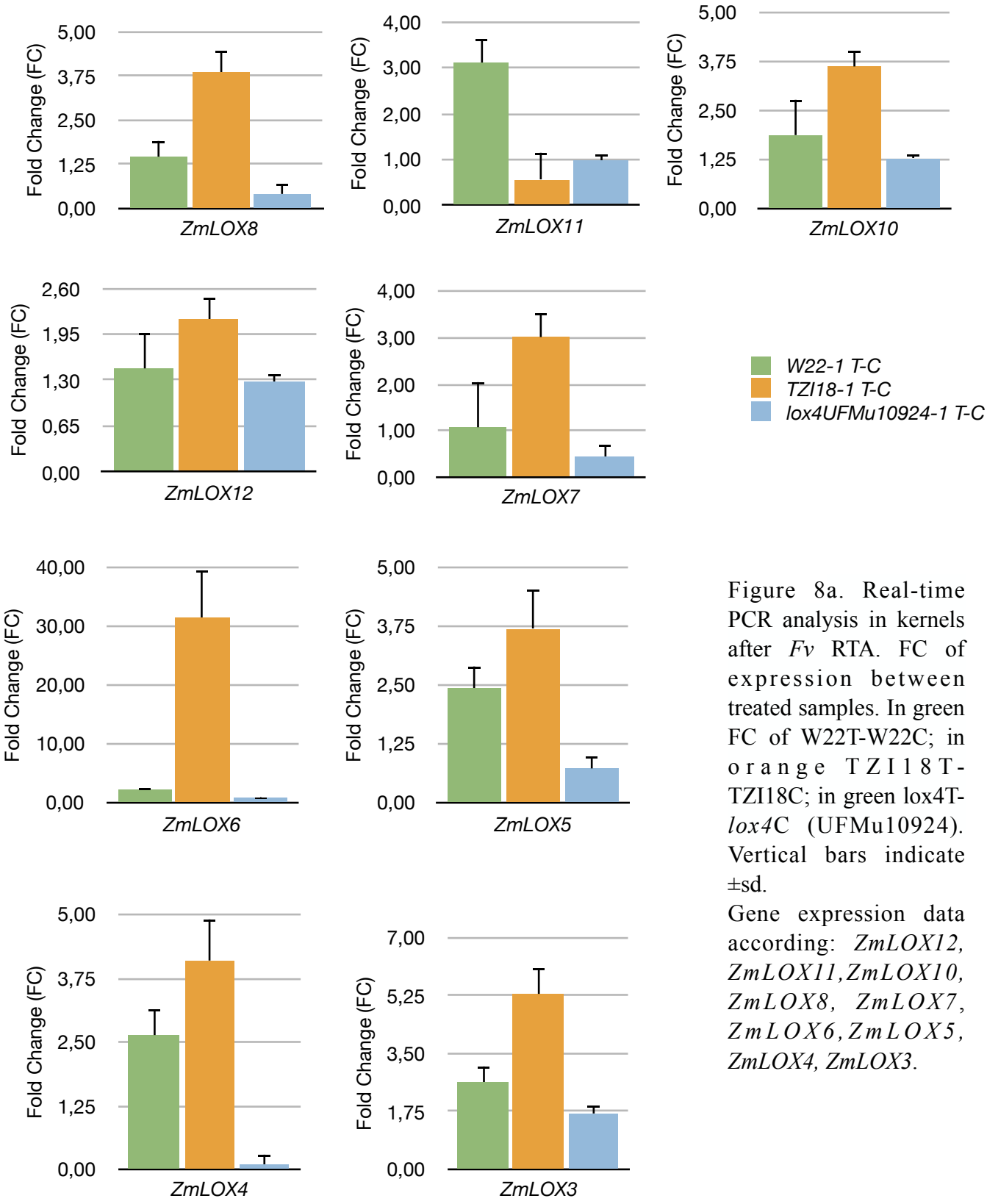

Figure 8a. Real-time PCR analysis in kernels after *Fv* RTA. FC of expression between treated samples. In green FC of W22T-W22C; in orange TZI18T-TZI18C; in green lox4T-*lox4*C (UFMu10924). Vertical bars indicate ±sd.
Gene expression data according: *ZmLOX12, ZmLOX11, ZmLOX10, ZmLOX8, ZmLOX7, ZmLOX6, ZmLOX5, ZmLOX4, ZmLOX3.*

Gene expression results - FC treated over control samples

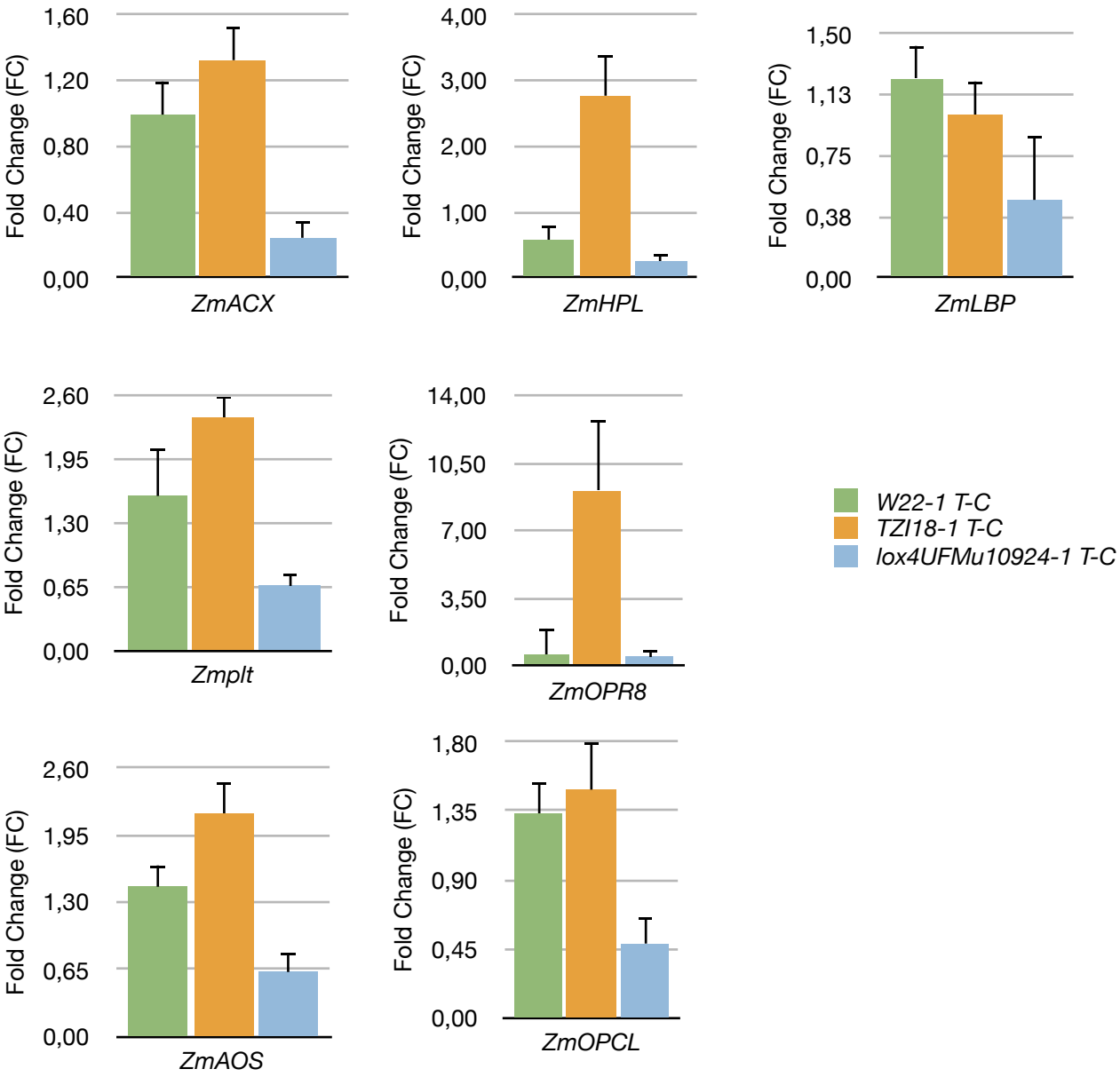

Figure 8b. Real-time RT-PCR analysis of GLV genes in kernels at 7 days after *Fv* inoculation by RTA. FC of expression between treated over control samples. In green FC of W22T-W22C; in orange TZI18T- TZI18C; in green lox4T-*lox4*C (UFMu10924). Vertical bars indicate ±sd. Gene expression data according: *Zm allene oxide synthase (ZmAOS)*, *Zm hydroperoxide lyase* (*ZmHPL)*, *Zm OPDA reductase8* (*ZmOPR8*), *Zm acyl-CoA oxidase,* (*ZmACX), Zm lipid binding protein* (*ZmLBP)*, *Zm phospholipid transfer protein,* (*Zmplt*), *OPC-8:0CoA ligase1* (*ZmOPCL)*.

Analysis of LOX activity

In order to gain some insights into maize lipoxygenase biochemistry, the two lines TZI18 and W22, and the UFMu*lox4* mutant (10924), already evaluated for disease resistance by RTA and the expression of genes for LOX and GLV pathway, were characterized by specific LOX activities by means of spectrophotometric techniques. The absorbance of each biologic replicate was measured in triple and a corresponding **ε** was calculated for each pH value. Linoleate hydroperoxidation activity was photometrically determined at 25°C and measurements of LOX activity corresponding to linoleate hydroperoxidation reaction (λ=234 nm) were calculated as reported in Pastore et al. (2000). The experiment was optimized for maize LOX extraction in phosphate buffer at pH 7.0 and the absorbance was calculated at pH 5.5. To explore LOX activity in different pH for extraction and absorbance different pH conditions were tested from pH 3.5 to 8.5, and the results are shown in Figure 9.

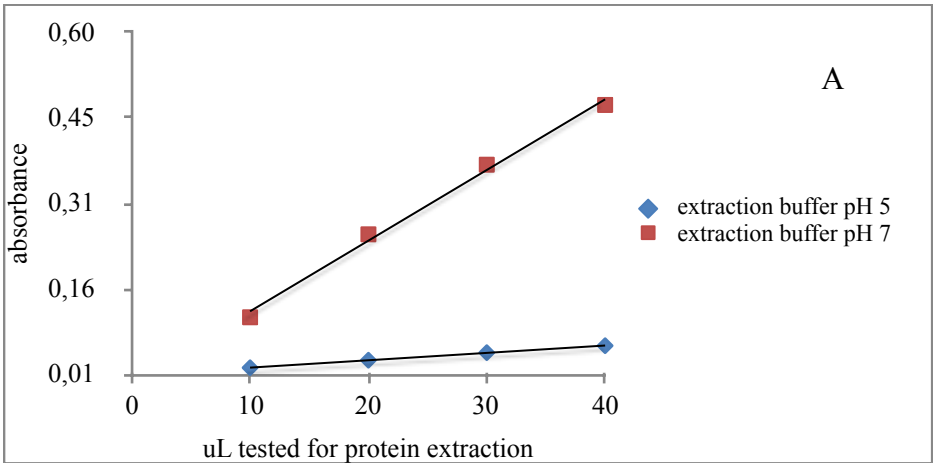

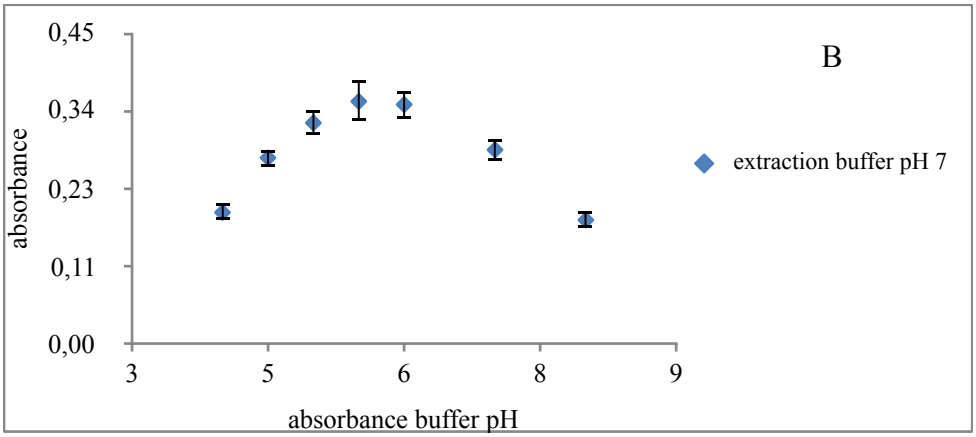

Figure 9. A. LOX activity explored at ph 5.0 (blue) and 7.0 (red). absorbance was measured for 10, 20, 30 and 40 uL of protein extraction. B. LOX activity explored for absorbance buffer from pH 3.5 to 8.0.

The results, expressed as UE/mg of protein extracted, showed that LOX activity was very low for the susceptible line W22 and UFMu*lox4* mutant both before and after the infection with *Fv* by RTA. In contrast with these findings, a different trend was observed for the line TZI18 that started from a higher basal level of enzymatic activities further increased by fungal treatment (0,232 UE/mg; Figure 10 and Table SD3). The low LOX content described for the UFMu*lox4* mutant probably reflects the reduced FC values observed for the LOX and GLV genes, and once again it points out the relevance of *ZmLOX4* gene in resistance mechanisms towards *Fv*. In a previous work by Battilani et al. (2018) it was depicted that without a functional *LOX4* seed did not accumulate normal levels of the jasmonic acid (JA) precursor, 12-oxo-phytodienoic acid (12-OPDA) or JA at basal levels. Remarkably, at 6 days after *Fv* infection, the *lox4* mutant was unable to accumulate any detectable level of 12-OPDA and less than half the normal level of JA compared with the wild type (Battilani et al., 2018). Taken together, these data suggested that the mutation in the gene *LOX4* caused the impaired LOX enzymatic activity and the consequent defective production of 9-oxylipin products, confirming the central role of this gene to induce normal JA biosynthesis after *F. verticillioides* infection in maize (Park et al., 2010; Battilani et al., 2018). Further analysis of the JA and oxylipin content will be carried out in UFMu*lox4* mutants to confirm these preliminary findings.

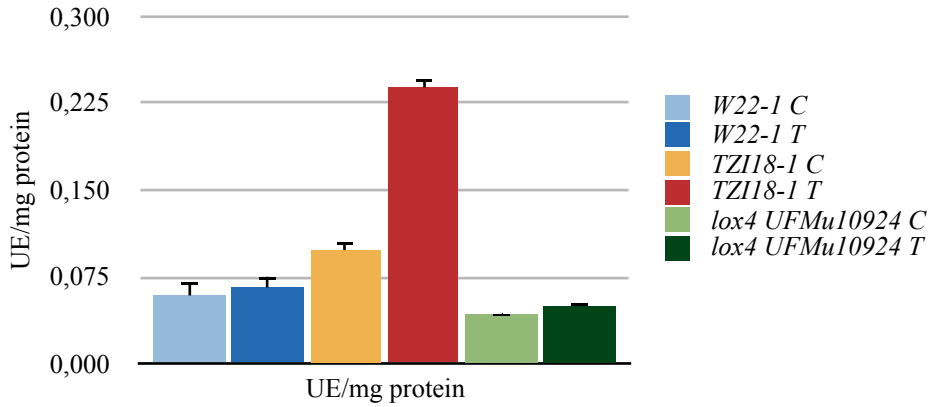

Figure 10. Total enzymatic LOX activity expressed as UE/mg of protein in W22 control (C) and treated (T), TZI18 C and T, and UFMu*lox4* 10924 C and T. Bars indicate ±sd.

Disease phenotyping by side-needle inoculation in field

Ears of TZI18, W22 and UFMu*lox4* mutant (10924) were inoculated in field with *Fv* using a side-needle inoculator in order to evaluate Fusarium ear rot resistance. Kernels were evaluated after 3 and 7 dpi for disease severity and showed clearly proof of susceptibility in the line W22 and the UFMu*lox4* mutant at both time-points, more pronounced at 7 dpi (Figure 11). As already observed through RTA and fumonisin analysis at seedling stage, UFMu*lox4* mutant was seriously affected by the disease also in adult plants under field conditions. These materials will be further evaluated for the expression analysis of *LOX* and *GLV* genes by real-time RT-PCR as well as for their lipidomic profile.

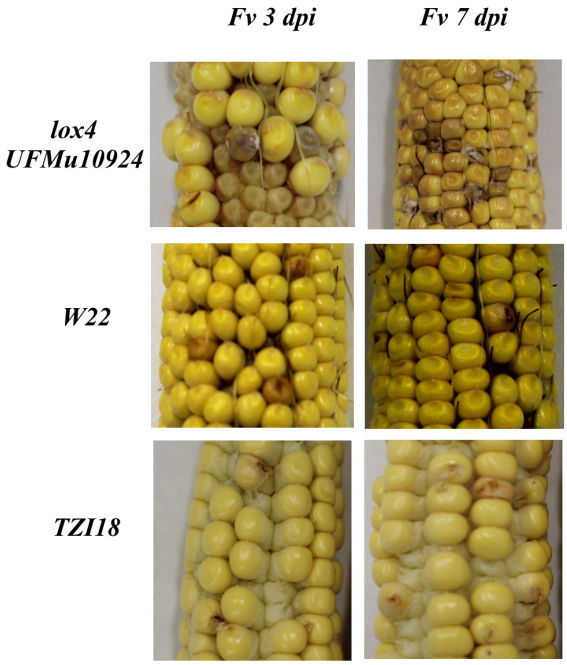

Figure 11. Ears of UFMu*lox4* mutant (10924), W22 (susceptible) and TZI18 (resistant) at 3 and 7 dpi with *Fv*.

Materials and methods

Maize inbred and growth conditions

The maize inbred W22 and TZI18 belong to the "Goodman" maize association population (Flint-Garcia et al., 2005) and were previously evaluated for *Fv* resistance resulting as susceptible and resistant lines, respectively (Stagnati et al., unpublished). Seeds were retrieved from USDA-ARS-NCRPIS (Iowa State University, Regional Plant Introduction Station, Ames, Iowa, United States, 50011-1170). The mutants UFMu*lox4* (*UFMu12283, UFMu06517, UFMu03075, UFMu10924, UFMu08535, UFMu03258, UFMu01831, UFMu11880, UFMu5366*) belong to the UFMu population available on Trasposon resource of MAIZEGDB and were retrieved as well. Mutator-transposable element insertional mutagenesis of UFMulox4 mutants was in the genetic background of the line W22. Inbred and mutants were maintained by sibling at the experimental farm Cerzoo set in Piacenza, Italy. Each maize genotype was grown in row 5 m long, with a distance of 80 cm between rows and 1 m between sectors. The sowing was made on April 6th 2017 for the first set of experiments and April 27th 2018 for the experiments regarding the disease phenotyping in field. Standard agricultural practices in the growing area (weed killers, fertilization and irrigation) were adopted. Fertilizer rates were applied as follow: 250 kg/ha N, 100 kg/ha P_2O_5 and 80 kg/ha K_2O.

Irrigation was applied by drip system in order to prevent water stress. Maize ears were hand-pollinated starting from the end of June for both years.

PCR confirmation of Mu insertions

To confirm the presence of Mu insertions in the *LOX4* gene, genomic DNA was extracted from individual plants and analyzed by PCR using gene-specific primers. At least two gene specific primers are required to be designed for each insertion (one upstream and one downstream of the insert site), and these need to be compatible with a Mu TIR specific primer available on MAIZEGDB. TIR8 was a mixture of four primers nested with respect to TIR6, allowing their use in two stages for enhanced specificity. TIR8 amplicons contain sufficient TIR sequence downstream of the primer to authenticate the Mu insertion. For sequence validation of insertion sites, an initial PCR reaction with TIR6 was carried out. Product was gel purified and sequenced using the nested TIR8 primer and/or gene-specific primer.

Additionally, pairs of 21-27 bp gene specific primers, with primers that anneal upstream and downstream of the predicted insert site were used. Ideally, the upstream and downstream gene specific primers should be separated by less than 500 bp in the wild type sequence to maximize amplification efficiency. Gene-specific primers that flanked the insertion site were first PCR-tested

in pairs with the wild type DNA from W22. This confirmed the capacity of the selected primers to amplify the expected wild type fragment.

Two step PCR conditions:

- 1. 94°C: 1 min
- 2. 94°C: 25 sec
- 3. 62°C: 30 sec
- 4. 72°C: 1 min (depends on expected size)
- 5. 8-10 cycles of 2 of 4
- 6. 94°C: 25 sec
- 7. 56°C: 30 sec
- 8. 72°C: 1 min (depends on expected size)
- 9. 26 cycles of 6 to 8
- 10. 72°C: 10 min
- 11. 4°C: pause

Sequencing of LOX4 gene fragment in UFMulox4 mutants and W22

Once the best primer pairs identified for *LOX4* gene in W22 control DNA and UFMu*lox4*, both forward and reverse primers were tested in combination with the TIR6 primer in the presence of DNA from individual UFMu plants. Parallel PCR reactions performed with the pair of flanking gene specific primers can be used to test for presence of the wild type allele and heterozygosity. However, amplification of a wild-type-sized fragment can sometimes occur even in situations where an insert is homozygous, if the gene is duplicated in the maize genome.

Experimental procedure of RTA assay

For each inbred (W22 and TZI18) and mutant UFMu*lox4*, seeds with similar size and shape, preferably flattened and without visible damage, were chosen for the experiment. To reduce as much as possible the presence of contaminating fungi, seeds were surface-sterilized by shaking in 50 mL tubes at room temperature with 70% EtOH for 5 min, sterile distilled water for 1 min, commercial bleach solution for 10 min and rinsed three times with sterile distilled water for 5 min each time (Christensen et al., 2012). Two towels of germinating paper (Anchor Paper, Saint Paul, Mn, USA) were moistened with sterilized distilled water. Ten seeds from a single inbred and mutant were placed on the germinating paper about 10 cm from the top of the towel with the embryo side facing out. Kernels were inoculated on the embryo side closed to the pedicel with 100 µL of $1x10^6$ conidial suspension of *F. verticillioides* ITEM10027 (MPVP 294). Another moistened towel was

placed over the inoculated seeds and the towels were rolled up and placed vertically in a 25L bucket covered with a plastic bag and incubated for 7 days at 25°C in the dark. Controls were prepared as previously described but avoiding the inoculation step. Inoculated and non-inoculated towels in the same bucket were inserted in open plastic bag to avoid cross-contamination. The steps of the experiment are shown in Figure 12.

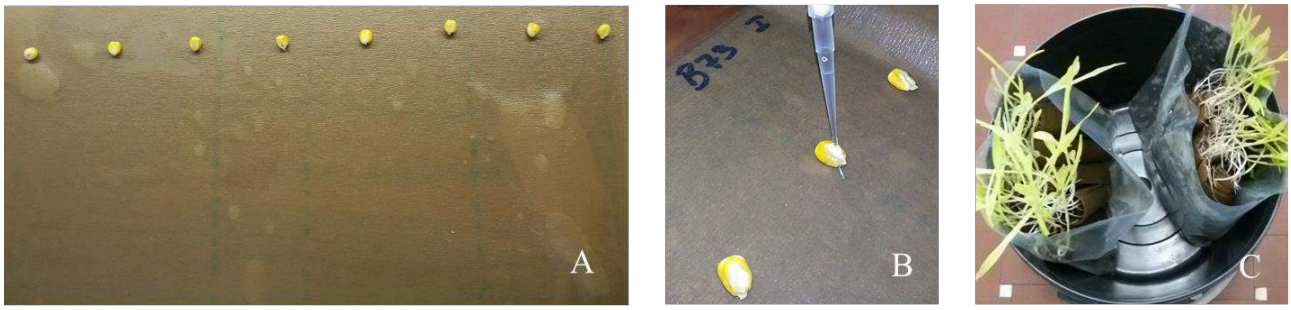

Figure 12. RTA assay A, positioning of kernels on germinating paper; B, seed inoculation; C, rolled towels after incubation.

Severity grid

Seedlings were rated adapting the 1-5 scale reported for soybean seedlings (Ellis et al., 2011), where 1 = healthy, germinated seedlings with no visible signs of colonization; 2 = germination and colonization of the kernel near the pedicel; 3 = germination with widespread colonization of the kernel and browning of the coleoptile; 4 = germination with reduced seedling development, complete colonization of the kernel, and lesions and abundant mold on the shoot; 5 = no germination due to complete rotting of the kernel (Figure 13). Seedling length was determined by measuring the length of the seed from the tip of the shoot to the tip of the root, in centimetres. Seedling weight was determined by measuring the weight of the whole germinated seed using a laboratory scale, in grams.

Figure 13. A, Five seedlings representing the different classes of the disease severity scale used to evaluate disease severity 7 days after *Fv* inoculation.

RNA isolation and real-time RT-PCR expression analysis

Total RNA extraction and purification were performed according to Maschietto et al. (2015). Real-time RT-PCR experiments were performed on kernels collected at 7 dpi using the 2× iQ SYBR Green Supermix (Bio-Rad, Hercules, CA, USA) and the CFX-96 device (Bio-Rad). 1 g of total RNA was used for cDNA synthesis following the iScript cDNA synthesis kit protocol (Bio-Rad). 20 ng of single strand cDNA determined by fluorometric assay (Qubit, Invitrogen) were used for real-time RT-PCR. Relative quantitative analysis was performed under the following conditions: 95 °C for 3 min and 40 cycles at 95 °C 15 s, 57-63 °C for 30 s. A melting curve analysis, ranging from 60 to 95 ° C with a 0.5 ° C increment for 5 s, was used to identify different amplicons, including non-specific products. Three technical replicates (within each biological replicate) were employed for each tested sample and template-free negative controls. Gene-specific primers were downloaded from literature or designed possibly within consecutive exons, separated by an intron, using Primer3 software (Table in supplemental data paragraph). Relative quantification of maize genes was

normalized to the housekeeping gene β-actin and FC values in gene expression were calculated using the $2^{-\Delta\Delta Ct}$ method (Schmittgen and Livak, 2008).

Lipoxygenase activity: oxydant enzyme activity

The lipoxygenase activity was estimated according to the method reported in Doderer et al. (1992). For each sample 1.5 g of maize flour was used to extract lipoxygenase protein in 3 mL of extraction buffer1 after 1 hour in ice agitation mix. Then the solution is centrifuged at 4 °C 35.000 g to 20 minutes. The surnatant obtains is used to measure lipoxygenase activity. Extraction buffer is a solution of potassium di-hydrogen orthophosphate (0.1 mM) and di- potassium hydrogen orthophosphate (0.1 mM) prepared by dissolving 13.6 and 17.4 g separately in distilled water, respectively, and volumes made up to one liter in each case. Both solutions were mixed in a ratio 16:84 and pH was adjusted to 7.5 and 100 ml of the solution, 0.186 g of ethylene diamine tetra acetic acid (EDTA) (0.5 mM) was added and used for enzyme extraction.

For the measurement of the lypoxigenase activity, the substrate solution was prepared by adding 35 µl of linoleic acid to 5 ml double distilled water containing 50 µl of Tween 20. The solution was kept at pH 9.0 by adding 0.2 M NaOH until all the linoleic acid was dissolved and the pH remained stable. After adjusting the pH to 7.0 by adding 0.2 MHCL, 0.1M phosphate buffer (pH 6.5) was added to a volume of 100 ml.

Lipoxygenase activity was measured by spectrophotometric assay in which the increase in extinction caused by the formation of the conjugated diene from linoleate, adding 50 µl of sample to 2.95 ml substrate solution. Absorbance was read at 234 nm and the activity was expressed as change in OD per min per mg protein in flour by using BSA as standard protein in Lowry's method (see next paragraph). The spectrophotometer used for the estimation of LOX activity and protein quantification is Perkin Elmer UV/VIS LAMBDA.

Estimation of protein by Lowry's method

The principle behind the Lowry's method of determining protein concentrations lies in the reactivity of the peptide nitrogen[s] with the copper [II] ions under alkaline conditions and the subsequent reduction of the Folin-Ciocalteay phosphomolybdic phosphotungstic acid to heteropolymolybdenum blue by the copper-catalyzed oxidation of aromatic acids (Dunn et al., 1992). This method is sensitive to pH changes and therefore, the pH of assay solution should be maintained at 10-10.5. This could be the major disadvantage of the method and for this reason very small volumes of sample with little or no effect on pH of the reaction mixture were used.

Furthermore, the Lowry's method is sensitive to low concentrations of protein, ranging from 0.10-2 mg of protein per ml.

Additionally, a variety of compounds may interfere with the Lowry procedure. These include some amino acid derivatives, certain buffers, drugs, lipids, sugars, salts, nucleic acids and sulphydryl reagents (Doderer et al., 1992).

Reagents:

A. 2% Na2CO3 in 0.1 N NaOH

B. 1% NaK Tartrate in H2O

C. 0.5% CuSO4.5 H2O in H2O

D. Reagent I: 48 ml of A, 1 ml of B, 1 ml C

E. Reagent II- 1 part Folin-Phenol [2 N]: 1 part water

(Perkin Elmer UV/VIS LAMBDA 45)

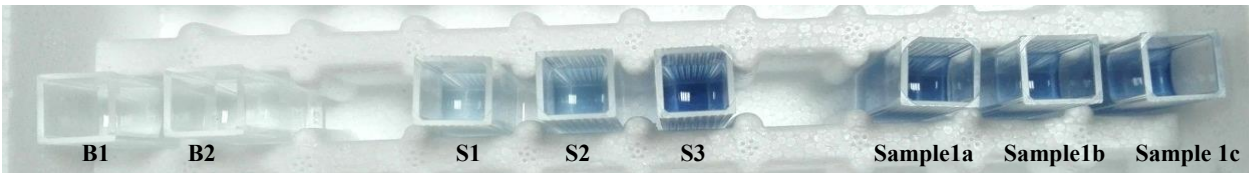

Figure 14. Estimation of protein by Lowry's Method. From the left to the right, the cuvettes relative to the whites (B1, B2), the BSA standard (S1, S2, S3) and the sample (Sample1a, Sample1b, Sample1c).

At the wavelength of 750 nm the two whites and the absorbances of standards (AS) and samples (AC) were read. Applying the formula1 the value of the ε (molar extinction coefficient relative to 1 mg of protein in 2.5 mL of solution) and the protein concentration (mg/mL) of the mother suspension is calculated using the formula 2:

• formula 1:

$$\boldsymbol{\varepsilon} = \frac{\left(\boldsymbol{AS}_1 * 2 + \boldsymbol{AS}_2 + \boldsymbol{AS}_3/2\right) * 100}{3}$$

where 100 = (1000 μg/mg) * (1/10 μg)

• formula 2:

$$\boldsymbol{Prot}\left(\boldsymbol{mg/mL}\right) = \frac{\left(\boldsymbol{AC}_1 + \boldsymbol{AC}_2 + \boldsymbol{AC}_3\right)}{3} * \frac{1}{\boldsymbol{\varepsilon}} * 200$$

where 200 takes into account the dilution factor.

The absorbance of the samples must be between those of the standards, where 200 takes into account the dilution factor.

Analysis of total fumonisin content by Fumo-V-AQUA test

5 g +/- 0.1 g of ground sample were weighed and placed in an extraction tube. 25 mL of AQUA buffer (VICAM, Milford, MA, USA) were measured with a graduated cylinder and poured it into the extraction tube. The extraction tube was covered and the mixture was vortexed for 2 minutes at max speed. The extract was then filtered into a clean extraction tube. For the total fumonisin quantification 100 µL of filtered extract were transferred to the Fumo-V strip test (VICAM) by dropping (~ 1 drop/second) vertically into the circular opening. After allowing strip test to develop for 5 minutes on a flat surface (such as a countertop), the Fumo-V strip test was inserted into the Vertu reader and results were read.

data available according RTA			Rolled Towel Assay			control						treated					
					Roll	Plant weight	stdev	Severity	stdev	Plant lenght	stdev	Plant weight	stdev	Severity	stdev	Plant lenght	stdev
			replicate	UFMulox4	susceptible												
fumonisin content	gene expression	lipoxygenase activity	replicate 1		W22-1	0,40	0,05	1,00	0,00	3,00	3,37	0,38	0,05	3,33	1,04	2,30	2,67
fumonisin content	gene expression	lipoxygenase activity	replicate 2		W22-2	0,71	0,17	2,48	1,02	18,30	7,03	0,71	0,17	2,48	1,02	18,30	7,03
fumonisin content	gene expression	lipoxygenase activity	replicate 3		W22-3	0,62	0,15	1	0,00	9,85	5,88	0,72	0,20	2	1,06	19,50	7,72
			replicate 1		W22-R 538	0,47	0,11	1,00	0,00	4,45	3,75	0,47	0,13	3,85	1,14	5,90	6,99
			replicate 2		W22-R 539	0,68	0,15	1,00	0,00	14,10	4,92	0,66	0,18	2,85	1,00	14,10	7,70
			replicate 1		A188-7	0,71	0,15	1	0,00	12,65	9,15	0,52	0,17	4,35	1,04	4,40	5,64
			replicate 2		A188-8	0,72	0,16	1	0,00	12,65	9,15	0,52	0,17	4,75	1,04	4,40	5,64
			replicate 3		A188-9	0,82	0,16	1	0,00	12,65	9,15	0,52	0,17	4,75	1,04	4,70	5,64
					resistant												
fumonisin content	gene expression	lipoxygenase activity	replicate 1		TZI18-1	0,91	0,38	1,225	0,90	22,05	9,01	0,97	0,18	1,65	0,28	24,75	5,08
fumonisin content	gene expression	lipoxygenase activity	replicate 2		TZI18-2	0,81	0,18	1,225	0,90	23,00	9,01	0,78	0,19	1,65	0,28	23,75	5,08
fumonisin content	gene expression	lipoxygenase activity	replicate 3		TZI18-3	0,78	0,15	1,225	0,90	22,00	9,01	0,87	0,18	1,65	0,28	22,75	5,08
					lox4												
fumonisin content	gene expression	lipoxygenase activity	replicate 1	UFMu10924	570-1	0,62	0,19	1	0,00	16,63	8,19	0,45	0,18	6,18	11,08	9,50	8,24
fumonisin content	gene expression	lipoxygenase activity	replicate 2	UFMu10924	570-2b	0,593	0,15	1,00	0,00	22,00	8,03	0,593	0,15	1,00	0,00	22,00	8,03
fumonisin content	gene expression	lipoxygenase activity	replicate 3	UFMu10924	570-2a	2,325	7,93	1,00	0,00	18,05	10,54	0,5275	0,23	3,60	1,03	16,50	11,22
			replicate 1	UFMu3258	576-1	0,46	0,23	1	0,00	6,80	8,88	0,62	0,19	3,28	1,33	14,60	9,42
			replicate 2	UFMu3258	576-2	0,4985	0,20	1,00	0,00	10,85	10,99	0,3775	0,13	4,43	0,73	5,70	7,96
			replicate 3	UFMu3258	576-3	0,7135	0,16	1,05	0,23	25,20	6,57	0,6265	0,21	3,50	1,01	18,25	12,22
			replicate 1	UFMu1831	566-2	0,42	0,18	1	0,00	10,30	9,74	0,43	0,13	8,65	15,89	8,30	8,55
			replicate 2	UFMu1831	566-4	0,77	0,09	1,00	0,00	24,85	4,58	0,7185	0,11	2,30	0,59	22,85	7,62
			replicate 3	UFMu1831	566-6	0,61	0,21	1,00	0,00	18,65	9,16	0,611	0,21	2,60	1,13	21,10	9,79
			replicate 1	UFMu11880	568-1	0,73	0,22	1,00	0,00	18,55	8,82	0,59	0,15	2,48	1,21	13,15	7,33
			replicate 2	UFMu11880	568-2a	0,74	0,19	1,00	0,00	27,30	7,08	0,6945	0,16	2,53	0,82	21,35	9,11
			replicate 3	UFMu11880	568-2b	0,7175	0,20	1,00	0,00	23,65	8,66	0,737	0,10	2,43	0,63	23,85	5,97
			replicate 1	UFMu5366	569-3	0,84	0,15	1	0,00	22,20	6,48	0,63	0,14	2,75	0,92	14,05	7,22
			replicate 2	UFMu5366	569-5	0,6925	0,14	1,00	0,00	24,35	4,88	0,805	0,11	2,90	0,42	23,90	6,98
			replicate 3	UFMu5366	569-4	0,7205	0,15	1,00	0,00	27,15	5,45	0,68	0,13	2,48	0,87	19,05	7,28
			replicate 1	UFMu12283	571-1	0,52	0,11	1,00	0,00	7,30	2,87	0,48	0,12	3,18	1,37	7,10	5,55
			replicate 2	UFMu12283	571-2	0,52	0,13	1,00	0,00	8,45	5,60	0,61	0,13	2,75	0,95	3,40	3,97
			replicate 3	UFMu12283	571-3	0,74	0,13	1,00	0,00	16,10	2,83	0,49	0,13	3,19	1,37	7,11	5,57
			replicate 1	UFMu6517	572-2	0,77	0,20	1	0,00	17,40	6,49	0,77	0,11	1,85	0,43	19,90	5,94
			replicate 2	UFMu6517	572-3	0,76	0,15	1,00	0,00	20,55	4,12	0,74	0,17	2,65	0,93	18,90	7,54
			replicate 3	UFMu6517	572-5	1,25	3,09	4,10	0,74	8,25	3,09	1,25	3,09	4,10	0,74	8,25	3,09
			replicate 1	UFMu3258	575-1	6,06	21,02	2,125	1,73	20,75	9,20	0,54	0,17	3,76	1,13	8,84	8,49
			replicate 2	UFMu3258	575-2	0,55	0,12	1,00	0,00	17,10	6,33	0,47	0,15	3,20	1,03	13,60	8,76
			replicate 1	UFMu8535	573-3	0,53	0,13	1,09	0,27	11,60	6,18	0,42	0,11	3,65	1,38	5,05	5,20
			replicate 2	UFMu8535	573-3a	0,62	0,14	1,05	0,23	14,45	4,94	0,58	0,15	2,90	0,97	14,05	7,01

Table SD1. RTA summary results of inbred lines tested. susceptible inbreds are showed in green, resistant in orange and *lox4* transposon alleles in blue. Each inbred has been tested in 3 biological replicate apart from UFMu3058 and UFMu8535. Control treatment (done with water); right side: *Fv* treatment 100 µL of $1x10^6$ conidial suspension of *Fv*.

Table SD2. Total fumonisin content of FB1, FB2 and FB3 in W22, TZI18 and UFMu10924 and UFMu3058 mutants.

SAMPLE RB	RT1 - PPM	RT2 - PPM	RT3 - PPM	AVERAGE RT	AVERAGE RB	DS
W22-C-1	0,00	0,41	0,01	0,14	0,29	0,36
W22-C-2	0,00	0,54	0,87	0,47		
W22-C-3	0,01	0,01	0,77	0,26		
W22-T-1	14,85	21,04	28,53	21,47	45,46	20,42
W22-T-2	75,65	42,04	50,07	55,92		
W22-T-3	55,03	60,87	61,07	58,99		
TZI18-C-1	1,00	0,00	0,87	0,62	0,33	0,47
TZI18-C-2	0,00	0,07	1,01	0,36		
TZI18-C-3	0,00	0,01	0,01	0,01		
TZI18-T-1	2,39	3,91	4,03	3,44	5,10	1,60
TZI18-T-2	7,71	5,01	4,75	5,82		
TZI18-T-3	5,32	6,80	6,00	6,04		
UFMu10924-C-1	0,02	0,00	0,01	0,01	0,02	0,02
UFMu10924-C-2	0,00	0,01	0,03	0,01		
UFMu10924-C-3	0,01	0,03	0,05	0,03		
UFMu10924-T-1	75,03	80,00	83,01	79,35	62,27	13,81
UFMu10924-T-2	47,01	48,08	50,07	48,39		
UFMu10924-T-3	57,57	58,87	60,83	59,09		
UFMu3258-C-1	0,00	0,01	0,34	0,12	1,20	1,87
UFMu3258-C-2	5,24	2,03	3,04	3,44		
UFMu3258-C-3	0,00	0,10	0,00	0,03		
UFMu3258-T-1	11,62	15,38	13,78	13,59	22,19	11,25
UFMu3258-T-2	37,38	35,01	37,10	36,50		
UFMu3258-T-3	10,00	18,00	21,47	16,49		

Table SD3. Total enzymatic LOX activity expressed as UE/mg of protein and UE/g dry weight in W22 control (C) and treated (T), TZI18 C and T, and UFMu*lox4* 10924 C and T.

sample	UE/mg prot. average	ds	UE/g dry weight average	ds
UFMu10924-1 C	0,050	0,002	1,2027	0,0469
UFMu10924-1 T	0,073	0,005	1,0455	0,0710
UFMu10924-2 C	0,022	0,001	0,4079	0,0254
UFMu10924-2 T	0,069	0,019	0,8890	0,2469
UFMu10924-2 C	0,071	0,003	1,2079	0,0428
UFMu10924-2 T	0,057	0,000	0,5188	0,0000
TZI18-1 C	0,066	0,002	0,8558	0,0260
TZI18-1 T	0,232	0,006	3,3809	0,0868
TZI18-2 C	0,057	0,001	1,1416	0,0148
TZI18-2 T	0,280	0,003	2,9110	0,0272
TZI18-3 C	0,070	0,001	1,0048	0,0131
TZI18-3 T	0,204	0,002	3,1413	0,0294
W22-1 C	0,114	0,001	1,4100	0,0147
W22-1 T	0,222	0,004	3,2863	0,0546
W22-2 C	0,023	0,003	0,3337	0,0367
W22-2 T	0,125	0,012	1,2735	0,1215
W22-3 C	0,092	0,001	1,6160	0,0244
W22-3 T	0,095	0,006	1,5579	0,0968

Table SD4. Sequence of primers used for real-time RT-PCR analyses. Ta= Annealing temperature; Zm= *Zea mays*.

Gene	**Primer Forward (5'→3')**	**Primer Reverse (5'→3')**	**T a (°C)**	**Source**
ZmLOX3	CGTTCCTCATCGACGTCAAC	GCGTGTAGACCTTGCTCTTG	57	AF329371.1
ZmLOX4	TACCGTGACACGCTGAACAT	CACAGCCACACCTCTCTTGA	57	DQ335762.1 Lanubile et al., 2014
ZmLOX5	CCGAGTTCTTCCTCAAGACG	CCTGGGAGTAGAGCTTGTGC	63	DQ335763.1 Lanubile et al., 2013
ZmLOX6	GTGTACACTCCACCGGACAG	GTTGAGCCAGTGAGTGACGA	57	DQ335764.1
ZmLOX7	GCAATCATGCCAGGCGAGGCGAGG	GAGCACGGCGACCGCGCCCGGCTC		*GRMZM2G070092, lox7, ts1b, Gramene*
ZmLOX8	AGATCCAGGAGAACAGCGAG	GATCATGGACGGAGGAGGAG	57	DQ335766.1
ZmLOX10	GACGAGTGCAACAACAACCT	TGCATGCTGAGGATGGATCA	57	DQ335768.1
ZmLOX11	TCGTGGTTCAAAGACGAGGA	ATCTCCTTTGTGATGGCGGA	57	DQ335769.1
ZmLOX12	AACAAGGGGTGTGCGTCTAC	TCATTGACGGAGACATGAGC	63	DQ335770.1
ZmAOS	GATGAGCAACGACTTCACGA	CACACGCACACACACAAAAA	57	NM_001111774.1 Lanubile et al., 2014
ZmOPR8	TACTGATGCCCGATGGATCC	AACCTGCTTTGATGGCGTTT	60	AY921645.1
ZmOPCL	GTGCCCATGTTCCACGTCTA	AGCATGGCGACGAGGATG	60	NM_001148670.1
ZmACX	GTCCTCGTCTTCCACGTTGT	CGAGGTCAAGACCAAAGCTC	57	GRMZM2G864319 Lanubile et al., 2014
Zmplt1	ATATCTATCCCGCCGTCGTC	TCCGTCTCCTCTCTCTCTCA	57	NM_001111841.1
ZmLBP	TTCGACACATCAAGCTTTGG	ACGCAAGCCATATCAGCTCT	57	GRMZM2G155555 Lanubile et al., 2014
ZmHPL	ATCTTCCGGTTCCTCTGCAA	AAGGAGTGGATGAGCAGCTC	60	AY540745.1
Zmβ-actin	ATGGTCAAGGCCGGTTTCG	TCAGGATGCCTCTCTTGGCC	57-63	AY273142.1 Lanubile et al., 2013

UFMu *lox4* primers pair for genotyping:

UFMu lox4	primer pair for LOX4 WT allele	primer pair for UFMu insertion
UFMu10924	pair: fL+rT=539bp	TIR6 + rT
UFMu3258	pair: fC+rT=539bp	TIR6 + fC
UFMu08535	pair: fL+rT=539bp	TIR6 + fL
UFMu3075	pair: fI+rO= 530bp	TIR6 + rO
UFMu06517	pair: fD + rM = 1087 bp	TIR6 +fD
UFMu12283	pair: fD + rM = 1087 bp	TIR6 + fD

name	sequence	Tm (C°)
UFMu insertion primers short version:		
TIR6	AGAGAAGCCAACGCCAWCGCCTCYATTTCGTC	71.7°
Mu insertion primers extended version:		
TIR6	AGAGAAGCCAACGCCAWCGCCTCYATTTCGTC	71.7° All
	AGAGAAGCCAACGCCAACGCCTCCATTTCGTC	
	AGAGAAGCCAACGCCATCGCCTCTATTTCGTC	
	AGAGAAGCCAACGCCAACGCCTCTATTTCGTC	
	AGAGAAGCCAACGCCATCGCCTCCATTTCGTC	
UFMu *lox4* primers sequences (5'—>3') and Tm (C°)		
fC	CTCTCAGTCATCATCGACTCAT	55
fD	CAGTCATCATCGACTCATCGTT	58
fI	CCTATGGAAGATTGGAAGTCGA	55
rM	ACAACTGTTCCATTCCATGTCC	57
rO	GCCATCTCAATCGCATTGAATG	56
fAD	AAGTACCCTGGACCCAAGTCAATAC	60
fAH	ACAAGAGCTGGAATTTCAACGAGC	60
fAL	CATTGAGCAGTAAACGCCTATAGC	57
rAQ	GAGTCGTTCACGCAGGCATAAG	59
rAU	TCCAGCTTCTTGTAGTCGTC	55

***UFMUlox4* sequences for transposon confirmation**

UFMu10924: primers: TIR6 + revT; sequenced with revT; sequence code FR07686682; transposon in blue.

CGAGTACAAAAGACCGAGGGGAGAATACTCACGTCGTTGGCGAGAAGACGCGTTCCTG
GGAGTAGAGATTGTGCGGGTAGATCCACGAGTTGGCGACGAAGACGACGGTGCCCCTG
CCGGGGACGCCCTCGAGGGTGAGCGACTTGAGGAAGAACTCGGCGTGCTGCAGGTTCC
TGACCAGGACGGCGCCCGGGACGCCCTGCGACCCGTCCCACTCGAAGCTCACCCGGTA
CAGAGATAATTGCCATTATAGACGAAGAGCGGACGGGATTCGACGAAATGGAGGCGATG
GCGCGGCTTCTCAGTGCGTCCAGTTGAGAGAGAACATTATCAAGAAAAATGAGACAAG
GCGGCTTAAATCTTATTCTAGGCGGGAGGTGTTATTATCCCCGAGGCGGCACACAGCACA
AAAGCTTGTAAGTTACTGTGCACCTCTCGGGTTAAAAGTTATGTGAAAAGTTTCATGTTT
TAGGAACATTCTTCTTCTCTTCTGCTTAACATGTTGCTCCTTTTTTTTCTTGCTCTTCTTCT
TCGTCTTCCCAACTTGTTCTTCCGTTTCTTATTTGAAGACAAAAAAAACCGGAGTAAGA
AGTGCTGACTTCTCTTTCATGACTTTCTGACCACCTAATCATAGGTAATGTAGTAGCTACT
GTTGCTTTTCTTCACTCCTCCCCCATTATCATATTTTCGGTTTCTTCTATAACCAATTGTTC
CTTTCTGAACCTTGTAGGATGTGAATTGTTGCAGCCAAAAAACTTGTTGATTGAGTCTGG
AAACGTCTCACTGATGAGGCCGCCCTTGCTTTTTGAGTCTTCCACCACCTAGATAAAAC
ACACACTTGATGGATGGGCAAGCAGTAACTTGCGT

UFMu12283: primers: TIR6 + forD; sequenced with forD; sequence code FR07686683; transposon in blue.

GTACCTCTTTTTTTTCACCTTTTCGTATACACGTCGCTGTCGCCTCCATCGCTGGGCTGGC
AAGAGAACGCGAGGCGAAGCAGCCGCGGCCGCCCGCCTATTTATCGCGAGATAATTGCC
ATTATGGACGAAGAGAGGAGGTGATTCGACGAAATGGAGGCGTTGGCGTTGGCTTCTCA
CAGATGTTAAGGTTGTCAACTCGAGGGGGGCACCCTGGACCACACCTGGGCATCCACTC
GTACGCCGTTTAGATTTTCTTCTTACAAAGGACCACTCACGGGCTTTTTCCAACCCCCAG
CTATGGCTACGCTTCCCTTGTTGATGATATATTGCCC

UFMu6517: primers: TIR6 + forD; sequenced with forD; sequence code FR07686686; transposon in blue.

GTCCGTCTTTTTTTTCACCTTTTCGTATACACGTCGCTGTCGCCTCCATCGCTGGGCTGGC
AAGAGAACGCGAGGCGAAGCAGCCGCGGCCGCCCGCCTATTTATCGCGGGCTCGCGGC
ACAGGGCAGCGGCAGTTCCATACATACATACACCAACCGTGCGTGAAGGAAGGCCTTTG
CTCGCCGCCACATCACATTGGCAGGCGAGGCGAGGGAGCGAGCAGCAGGGCAAGGCAT
CCACACCCACACCCACGAGATAATTGCCATTATAGACGAAGAGCGGACGGGATTCGACG
AAATGGAGGCGTTGGCTGAGCTTCTCTTGACG

UFMu3258: primers: TIR6 + forD; sequenced with forD; sequence code FR07686690; transposon in blue.

GACTTCTTTTTCATTTCTGTCCGGGGTTCGGGTTCCCAGGTTCCCAGTTCACACTTGAGG
GGTGGGCCCTATCGCCCTCTCCATTCCATGCGGCCGGCTGTTTTTTTTCGAGCAGTTTGC
CCCACCACTCTTACCTGTAACATGTTCCTTATTACACCGGAGGGCTGTCGCTTGAACCCT
TTGAGGCATGCTCTCCTGGTTAACAATTGCTTTGGTTGGTATGCCTTTGTGCATGTCAAC
GGACACTTTCACCTCACACATGCCTTTTAGACTGGATGGGATTGTAGACCACGGATACGT
CAGAATCGTTGAATGATTTATGGGAAGCACTCCGAACATCTTACCGTCACCATCATGATA
AGAAATCCCCTGACTTTTTCCATAAACGACTTATAAATCCTCGTGCCATATTGCACTATAT
AAGACCTTTCGTGGGAGTCAGACAATCTTGGGTAAGAACTTTAATGTGGTGGAAAACTA
CTCACCGCACGCTTTTAGAAATTAAGATCAAGACTGTACAGGGCATATGGAGATTTTTAA
AACTATTTGAGAGTGATACTCATTATACCCCACTCGTAGAATTGCTGCTACGTGATCTTTA
GGATCAGCCGATGGACGAACACAGAAGAATCCCCCCAACATAATCTCGCTGAGCATGTA
GGCCGAGTCTTCCCCCCTCCACACCCCAGGCAGTTTCGACACATAAGAGGTAGCTAAAC
AAGAAAATCGCATGTAGGTAGACATCAACTGTGAGAGTCATGCTTGCGATTGATGAGTA
GTGATCATCGCCAGCAATCAAACCTGACCGGCAAGTACCCCCGCATCCTAGGAGCCCAG
ATTGAATACTAATA

UFMu3075: primers: TIR6 + forC; sequenced with forC; sequence code FR07686692; transposon in blue.

GGTAACTTACTTTTTTTTCACCTTTTCGTATACACGTCGCTGTCGCCTCCATCGCTGGGCT
GGCAAGAGAACGCGAGGCGAAGCAGCCGCGGCCGCCCGCCTATTTATCGCGAGATAATT
GCCATTATGGACGAAGAGAGGAGGTGATTCGACGAAATGGAGGCGTTGGCGTTGGCTT
CTCACAGGCGGAGCTGCTGGTTAATCATACCTTTAAGTTGTCTGCAAAAAGATGTCAGC
GGAAGCGGCACCGCACAGGGCGGTTTGTGGTTGGTTCCCATTGATACCTTGCATAGTGC
TAGCTTCTTGATTAGATCCACGTAAAGCACACTGATGATCAAAGTCACCTACGTTAACTT
CCCATTAGCCCACACCTCCTCCTCCAACGACTTATACATAAGCGTGCAATATTGAACTCC
AAAAGACGGTAGATTGGAGTAATCCAAATTTAGAAATGAACTTGTCAGCGGGTCCTCCA
CTCGTGGACCCAGGTTGTTGGAAGTACACGTGGAGAGTGTACATTGCATATTGTGATTCC
CCCAGAACACTTCAGTGTGACATCACTCTCTCCATAAAATATACTAGCTATCGATCCCCAT
CTGTAGATTAGTCACTGTGTAAGCTGACTCCGGACACCAGACATACTTCCCTGATACTGT
CGAGTAGACACGTTGCTCTTGGTAGACCGGCACATAGGCTAGATGCGATGACGCAGACG
ATTCGCAGGGGTGATGAGCGCGCAGCGCATCTACCTCCTGAAGTTTGAGTTATGTTTTAT
TTTTCTAACTGTCGGTAGATCGAATAAGAGCTAGCAGCTCAGAGAATACTAGTTGACGA

UFMu8535: primers: TIR6 + revU; sequenced with revU; sequence code FR07686696; transposon in blue

GCACTTTAATTCGAGGTTGGTGGAGATGGTGTCTGTGATGTAGAGGATAACTTTGTCAGC
GGTGCAGCTGGTAAATGTGTTTCACGAGCAGGACGTATCCCAGGTGAGCCAGCCCACG
GTCATCTTCGGCTATGCCAACAGCAACGCCAACCCCATCGTACATGGTGCAGAGAAGCC
AACGCCAACGCCTCCATTTCGTCGAATCCCTTCCGCTCTTCGTCTATAATGGCAATTATCT
CGTCCCCGGCAGGGGCACCGTCGTCTTCGTCGCCAACTCGTGGATCTACCCGCACAATC
TCTACTCCCAGGAACGCGTCTTCTTCGCCAACGACGTGAGTATTCTTCCCCTTCGGTTTC
TTTTTTGGGTTCGCTGGCGACGTGAGTATCTACTCAGATAC

References

Brijesh K., Avinash Tiwari, Y. S. Saharawat, (2015) Lipoxygenase (LOX) Enzyme Activity of Wheat during Grain Filling Period under Conservation Agriculture Management. *Int Jour Plant Biotech.* Vol 1: 11.

Bate, N.J. and Rothstein, S.J. (1998). C6-volatiles derived from the lipoxygenase pathway induce a subset of defense-related genes. *Plant J.* 16: 561–569.

Battilani P., Lanubile A., Scala V., Reverberi M., Gregori R., Falavigna C., Dall'Asta C., Park Y.S., Bennet J., Borrego E.J., Kolomiets M. (2018). Oxylipins from both pathogen and host antagonize jasmonic acid-mediated defence via the 9-lipoxygenase pathway in Fusarium verticillioides infection of maize. *Mol Plan Pathol.* 19(9), 2162–2176.

Blée E. (2002). Impact of phyto-oxylipins in plant defense. *Trends Plant Sci.* 7:315-321.

Chen, G., Hackett, R., Walker, D., Taylor, A., Lin, Z., and Grierson, D. (2004). Identification of a specific isoform of tomato lipoxygenase (TomloxC) involved in the generation of fatty acid-derived flavor compounds. Plant Physiol. 136: 2641–2651.

Christensen S.A., Huffaker A., Kaplan F., Sims J., Ziemann S., Doehlemann G., Ji L., Schmitz R.J., Kolomiets M.V., Alborn H.T., et al. (2015). Maize death acids, 9-lipoxygenase-derived cyclopente(a)nones, display activity as cytotoxic phytoalexins and transcriptional mediators. *Proc Natl Acad Sci USA.* 112: 11407–11412.

Christensen, S.A., Nemchenko, A., Borrego, E., Murray, I., Sobhy, I.S., et al., (2013). The maize lipoxygenase, *ZmLOX10*, mediates green leaf volatile, jasmonate and herbivore-induced plant volatile production for defense against insect attack. *Plant J.* 74, 59–73.

Christensen, S.A., Nemchenko, A., Park, Y., Borrego, E., Huang, P., Schmelz, E.A., et al., (2014). The novel monocot-specific 9-lipoxygenase *ZmLOX12* is required to mount an effective jasmonate-mediated defense against *Fusarium verticillioides* in maize. *Mol. Plant Microbe Interact*. 27, 1263–1276.

D'Auria, J.C., Chen, F., and Pichersky, E. (2002). Characterization of an acyltransferase capable of synthesizing benzylbenzoate and other volatile esters in flowers and damaged leaves of Clarkia breweri. *Plant Physiol*. 130: 466-476.

De La Fuente, G.N., Murray, S.C., Isakeit, T., Park, Y.S., Yan, Y., Warburton, M.L., Kolomiets, M.V., (2013). Characterization of genetic diversity and linkage disequilibrium of *ZmLOX4* and *ZmLOX5* loci in maize. *PLoS One* 8 (1), e53973.

Doderer A, Kokkelink I, van der Veen S, *et al.* (1992) Purification and Characterization of Two Lipoxygenase Isoenzymes from Germinating Barley. *Biochim. Biophys. Acta.*; 1120: 97–104p.

Dolezal, A.L., Shu, X., Obrian, G.R., Nielsen, D.M., Woloshuk, C.P., Boston, R.S., Payne, G.A., (2014). Aspergillus flavus infection induces transcriptional and physical changes in developing maize kernels. *Front. Microbiol*. 5, 1–10.

Dombrecht, B., Gang, P.X., Sprague, S.J., Kirkegaard, J.A., Ross, J.J., Reid, J.B., et al., (2007). MYC2 differentially modulates diverse jasmonate-dependent functions in *Arabidopsis. Plant Cell* 19, 2225–2245.

Ellis M. L., Broders K. D., Paul P. A., Dorrance A. E. (2011). Infection of Soybean Seed by *Fusarium graminearum* and Effect of Seed Treatments on Disease Under Controlled Conditions. *Phytopathology.* vol95, issue 4 401-407. 39.

Ellis M. L., Cruz Jimenez D. R., Leandro L. F., and Munkvold G. P. (2014). Genotypic and phenotypic characterization of fungi in the *Fusarium oxysporum* species complex from soybean roots. *Phytopathology* 104:1329-1339.

Engelberth, J., Alborn, H.T., Schmelz, E.A., and Tumlinson, J.H. (2004). Airborne signals prime plants against insect herbivore attack. Proc. Natl. Acad. Sci. USA 101: 1781-1785.

Feussner, I. and Wasternack, C. (2002) The lipoxygenase pathway. *Annu. Rev. Plant Biol.* 53, 275–297.

Flint-Garcia S.A., Thuillet A.C., Yu J., Pressoir G., Romero S.M., Mitchell S.E., Doebley J., Kresovich S., Goodman M.M., Buckler E.S. (2005). Maize association population: a high- resolution platform for quantitative trait locus dissection. *Plant Journal.* 44(6):1054-64

Gao, X., Brodhagen, M., Isakeit, T., Brown, S.H., Göbel, C., Betran, J., et al., (2009). Inactivation of the lipoxygenase ZmLOX3 increases susceptibility of maize to *Aspergillus spp*. *Mol. Plant Microbe Interact.* 22, 222–231.

Gao, X., Shim, W.B., Göbel, C., Kunze, S., Feussner, I., Meeley, R., et al., (2007). Disruption of a maize 9-lipoxygenase results in increased resistance to fungal pathogens and reduced levels of contamination with mycotoxin fumonisin. *Mol. Plant Microbe Interact.* 20, 922–933.

Gao, X., Starr, J., Göbel, C., Engelberth, J., Feussner, I., Tumlinson, J., Kolomiets, M., (2008a). Maize 9-lipoxygenase ZmLOX3 controls development, root-specific expression of defense genes, and resistance to root-knot nematodes. *Mol. Plant Microbe Interact.* 21, 98–109.

Gao, X., Stumpe, M., Feussner, I., Kolomiets, M.V., (2008b). A novel plastidial lipoxygenase of maize (Zea mays) *ZmLOX6* encodes for a fatty acid hydroperoxide lyase and is uniquely regualted by phytohormones and pathogen infection. *Planta* 227, 491–503.

Halitschke, R., Ziegler, J., Keinanen, M. and Baldwin, I.T. (2004). Silencing of hydroperoxide lyase and allene oxide synthase reveals substrate and defense signaling crosstalk in Nicotiana attenuata. *Plant J*. 40: 35–46.

Hamberg, M. (2000). New cyclopentenone fatty acids formed from linoleic and linolenic acids in potato. Lipids 35: 353-63.

Howe, G., and Jander, G. (2008). Plant immunity to insect herbivores. *Annu. Rev. Plant Biol*. 59: 41-66.

Jat R.K., Sapkota TB, Singh Ravi G, *et al* (2014). Seven Years of Conservation Agriculture in a Rice–Wheat Rotation of Eastern Gangetic Plains of South Asia: Yield Trends and Economic Profitability. *Field Crops Res.*; 164: 199–210p.

Lanubile, A., Logrieco, A., Battilani, P., Proctor, R. H., and Marocco, A. (2013). Transcriptional changes in developing maize kernels in response to fumonisin-producing and nonproducing strains of Fusarium verticillioides. *Plant Sci*. 210:183-192.

Lanubile, A., Pasini, L., Marocco, A., (2010). Differential gene expression in kernels and silks of maize lines with contrasting levels of ear rot resistance after *Fusarium verticillioides* infection. *J. Plant Physiol.* 167, 1398–1406.

Lanubile, A., Pasini, L., Lo Pinto, M., Battilani, P., Prandini, A., and Marocco, A. (2011). Evaluation of broad spectrum sources of resistance to *Fusarium verticillioides* and advanced maize breeding lines. *World Mycotoxin J.* 1, 43–51. doi: 10.3920/WMJ2010.1206

Lanubile, A., Maschietto, V., De Leonardis, S., Battilani, P., Paciolla, C., Marocco, A., (2015). Defense responses to mycotoxin-producing fungi *Fusarium proliferatum, F. subglutinans,* and *Aspergillus flavus* in kernels of susceptible and resistant maize genotypes. *Mol. Plant Microbe Interact*. 28, 546–557.

Leon, J., Royo, J., Vancanneyt, G., Sanz, C., Silkowski, H., Griffiths, G., and Sanchez-Serrano, J.J. (2002). Lipoxygenase H1 gene silencing reveals a specific role in supplying fatty acid hydroperoxides for aliphatic aldehyde production. *J. Biol. Chem.* 277: 416–423.

Lorenzo, O., Chico, J.M., Sánchez-Serrano, J.J., Solano, R., 2004. JASMONATE-INSENSITIVE1 encodes a MYC transcription factor essential to discriminate between different jasmonate-regulated defense responses in *Arabidopsis. Plant Cell* 16, 1938–1950.

Maschietto, V., Marocco, A., Malachova, A., and Lanubile, A. (2015). Resistance to *Fusarium verticillioides* and fumonisin accumulation in maize inbred lines involves an earlier and enhanced expression of lipoxygenase (*LOX*) genes. *J. Plant Physiol.* 188, 9–18.

Matsui K. (2006). Green leaf volatiles: Hydroperoxide lyase pathway of oxylipin metabolism. Curr. Opin. in Plant Biol. 9: 274–280.

McCarty DR, Suzuki M, Hunter C, Koch KE. (2013). Genetic and molecular analysis of Uniform Mutransposon insertion lines. *Methods Mol Biol*, 1057:157–166.

McCarty DR, Settles AM, Suzuki M, Tan BC, Latshaw S, Porch T, Robin K, Baier J, Avigne W, Lai J, Messing J, Koch KE, Hannah LC. (2005) Steady-state transposon mutagenesis in inbred maize. *Plant J.* 44:52-61.

McCarty DR, Meeley RB. (2009) Transposon resources for forward and reverse genetics in maize. In. Handbook of Maize: genetics and genomics. (Ed. JL Bennetzen, S. Hake). *Springer Science Berlin.* pp 561-584.Christensen, S.A., Kolomiets, M.V., 2011. The lipid language of plant-fungal interactions. *Fungal Genet. Biol.* 48, 4–14.

Ogorodnikova A.V., Gorina, S.S., Mukhtarova L.S., Mukhitova F.K., Toporkova Y.Y., Hamberg M., Grechkin A.N. (2015). Stereospecific biosynthesis of (9*S*,13*S*)-10- oxophytoenoic acid in young maize roots. *Biochim. Biophys. Acta Mol. Cell Biol. Lipids.* 185, 1262–1270.

Park, Y.S., Kunze, S., Ni, X., Feussner, I., Kolomiets, M.V., (2010). Comparative molecular and biochemical characterization of segmentally duplicated 9-lipoxygenase genes *ZmLOX4* and *ZmLOX5* of maize. *Planta* 231, 1425–1437.

Prost, I., Vicente, J., Rodriguez, M.J., Carbonne, F., Griffiths, G., Tugaye, M.T.E., Rosahl, S., Castresana, C., Hamberg, M., and Fournier, J. (2005). Evaluation of the antimicrobial activities of plant oxylipins supports their involvement in defense against pathogens. *Plant Physiol.* 139: 1902–1913

Reid, L.M., Zhu, X., Parker, A., Yan, W., (2009). Increased resistance to Ustilago zeae and Fusarium verticilliodes in maize inbred lines bred for Fusarium graminearum resistance. *Euphytica* 165, 567–578.

Scala, V., Giorni, P., Cirlini, M., Ludovici, M., Visentin, I., Cardinale, F., Fabbri, A.A., Fanelli, C., Reverberi, M., Battilani, P., Galaverna, G. and Dall'Asta, C. (2014) LDS1 produced oxylipins are negative regulators of growth, conidiation and fumonisin synthesis in the fungal maize pathogen Fusarium verticillioides. *Front. Microbiol.* 5, 669.

Schmittgen, T.D., Livak, K.J., (2008). Analyzing real-time PCR data by the comparative CT method. *Nat. Protoc.* 3, 1101–1108.

Vancanneyt, G., Sanz, C., Farmaki, T., Paneque, M., Ortego, F., Castanera, P., and Sanchez-Serrano, J.J. (2001). Hydroperoxide lyase depletion in transgenic potato plants leads to an increase in aphid performance. *Proc. Natl. Acad. Sci.* USA 98: 8139–8144.

Wasternack C. (2007). Jasmonates: An update on biosynthesis, signal transduction and action in plant stress response, growth, and development. *Ann. of Bot*. 100: 681-687

Wilson R.A., Gardner H.W., Keller N.P. (2001). Cultivar-dependent expression of a maize lipoxygenase responsive to seed infesting fungi. *Mol. Plant Microbe Interact*. 14, 980–987.

Yan Y., Christensen S., Isakeit T., Engelberth J., Meeley R., Hayward A., Emery R. J., and Kolomiets M. V. (2012). Disruption of OPR7 and OPR8 reveals the versatile functions of jasmonic acid in maize development and defense. *Plant Cell.* 24:1420-1436.

Yeats, T.H., Rose, J.K.C., 2008. The biochemistry and biology of extracellular plant lipid-transfer proteins (LTPs). *Protein Sci.: Publ. Protein Soc.* 17, 191–198.